

Distributed Adaptive Learning with Multiple Kernels in Diffusion Networks

Ban-Sok Shin, *Student Member, IEEE*, Masahiro Yukawa, *Member, IEEE*, Renato L. G. Cavalcante, *Member, IEEE*, and Armin Dekorsy, *Member, IEEE*

Abstract—We present an adaptive learning scheme for the distributed identification of nonlinear systems with a network of nodes. The proposed algorithm consists of a local adaptation stage utilizing multiple kernels with projections onto hyperslabs and a diffusion stage to achieve consensus over the whole network. Multiple kernels are incorporated to enhance the approximation of functions with several high and low frequency components common in practical scenarios. We provide a thorough convergence analysis of the proposed scheme based on the metric of the Cartesian product of multiple reproducing kernel Hilbert spaces. To this end, we introduce a modified consensus matrix considering this specific metric and prove its equivalence to the ordinary consensus matrix. The use of hyperslabs allows to significantly reduce the communication overhead in the network with only minor losses in the error performance. Numerical evaluations with synthetic and real data are conducted showing the efficacy of the proposed scheme compared to the state of the art schemes.

Index Terms—Distributed adaptive learning, kernel adaptive filter, multiple kernels, consensus, spatial reconstruction, nonlinear regression

I. INTRODUCTION

DISTRIBUTED learning in networks is a topic of high importance due to its applicability in various areas such as environmental monitoring, social networks and big data [1]–[3]. In such applications, observed data are usually spread over the nodes, and thus, they are unavailable at a central entity. In environmental monitoring applications, for instance, nodes observe a common physical quantity of interest such as temperature, gas or humidity at each specific location. The objective for each node is to achieve a spatial reconstruction of the physical quantity over the area covered by the network. Therefore, distributed learning algorithms are required to exploit the observations available in the network based on information exchanges among neighboring nodes.

For the distributed identification of linear systems a variety of algorithms have been proposed in the past decade, see for example [4]–[12]. In contrast to these works, in this paper we address the problem of distributed learning of *nonlinear functions or systems*. To this end, we exploit kernel methods,

which have been used to solve e.g. nonlinear system identification tasks [13], [14]. Based on a problem formulation in a reproducing kernel Hilbert space (RKHS) linear techniques can be applied to identify an unknown nonlinear system. This system is then modeled as an element of the RKHS, and corresponding kernel functions are utilized for its approximation. This methodology has been exploited to derive kernel adaptive filters which are suited for nonlinear system identification tasks [15]–[25]. A variety of algorithms have been derived and studied in the literature such as the naive online regularized risk minimization [15], the kernel normalized least-mean-squares, the kernel affine projection [20] or the hyperplane projection along affine subspace (HYPASS) [23], [26]. These algorithms enjoy significant attention due to their limited complexity and their applicability in online learning scenarios. The HYPASS algorithm has been derived from a functional space approach based on the adaptive projected subgradient method (APSM) [27] in the set-theoretic estimation framework [28], [29]. It exploits a metric with regard to the kernel Gram matrix showing faster convergence and improved steady-state performance. The kernel Gram matrix determines the metric of an RKHS and is thus decisive for the convergence behavior of gradient-descent algorithms [30]. In [31], [32] kernel adaptive filters have been extended by multiple kernels to increase the degree of freedom in the estimation process. By this, a more accurate approximation of functions with several high and low frequency components is possible with a smaller number of dictionary samples compared to using a single kernel only.

Regarding distributed kernel-based estimation algorithms, several schemes have been derived such as [33]–[41]. In [33] a distributed consensus-based regression algorithm based on kernel least squares has been proposed and extended by multiple kernels [34]. Both schemes utilize alternating direction method of multipliers (ADMM) [42] for distributed processing and a consensus constraint guaranteeing convergence to the same coefficient vector at all nodes. However, this approach only considers a distributed regression based on a fixed set or a *batch* of input-output pairs which do not change over time. Therefore, no sequential processing is operated within the network. The schemes proposed in [38], [39] follow the approach of incremental updates based on the kernel least-mean-squares (KLMS) within a network of nodes. Here, the KLMS update is performed sequentially over the nodes which does not allow for parallel processing and thus prohibits strict consensus among the nodes. Recent works in [35]–[37] apply diffusion-based schemes to the KLMS to derive distributed kernel adaptive filters where nodes process

B.-S. Shin and A. Dekorsy are with the Department of Communications Engineering, University of Bremen, Germany, e-mails: shin@ant.uni-bremen.de, dekorsy@ant.uni-bremen.de.

M. Yukawa is with the Department of Electronics and Electrical Engineering, Keio University, Yokohama, Japan, e-mail: yukawa@elec.keio.ac.jp.

R.L.G. Cavalcante is with the Fraunhofer Heinrich Hertz Institute, Berlin, Germany, e-mail: renato.cavalcante@hhi.fraunhofer.de.

M. Yukawa is thankful to JSPS Grants-in-Aid (15K06081, 15K13986, 15H02757).

information in parallel. The functional adapt-then-combine KLMS (FATC-KLMS) proposed in [35] is a kernelized version of the linear adapt-then-combine diffusion least-mean-squares (ATC-DLMS) from [9]. The random Fourier features diffusion KLMS (RFF-DKLS) proposed in [36] uses random Fourier features to achieve a fixed-size coefficient vector and to avoid an a priori design of a dictionary set. However, the achievable performance strongly depends on the number of utilized Fourier features. Besides, the aforementioned schemes incorporate update equations in the ordinary Euclidean space and thus, do not exploit the more suitable metric induced by the kernel Gram matrix. Furthermore, the majority of these schemes do not consider multiple kernels in their adaptation mechanism.

In this paper, we propose a distributed kernel adaptive filtering scheme with multiple kernels based on the Cartesian HYPASS (CHYPASS) from [32] and on average consensus. In contrast to state of the art schemes, we formulate the optimization problem incorporating the metric induced by the kernel Gram matrix based on multiple kernels, and we exploit projections induced by this specific metric yielding significant gains in performance. For the theoretical analysis of the proposed algorithm we need to consider this metric and thus introduce a *modified consensus matrix* operating in the kernel metric. We prove that this matrix is equivalent to the ordinary consensus matrix as used in [10] and provide a corresponding convergence analysis. Furthermore, we demonstrate that by projecting the current estimate onto a *hyperslab* instead of an ordinary hyperplane we can significantly reduce the communication overhead in the network and the computational demand per node. We corroborate our findings by numerical evaluations on synthetic as well as real data and by proofs given in the appendices.

II. PRELIMINARIES

A. Basic Definitions

We denote the inner product and the norm of the Euclidean space \mathbb{R}^M by $\langle \cdot, \cdot \rangle_{\mathbb{R}^M}$ and $\|\cdot\|_{\mathbb{R}^M}$, respectively, and those in the RKHS \mathcal{H} by $\langle \cdot, \cdot \rangle_{\mathcal{H}}$ and $\|\cdot\|_{\mathcal{H}}$, respectively. Given a positive definite matrix $\mathbf{K} \in \mathbb{R}^{M \times M}$, $\langle \mathbf{x}, \mathbf{y} \rangle_{\mathbf{K}} := \mathbf{x}^T \mathbf{K} \mathbf{y}$, $\mathbf{x}, \mathbf{y} \in \mathbb{R}^M$, defines an inner product with the norm $\|\mathbf{x}\|_{\mathbf{K}} := \sqrt{\langle \mathbf{x}, \mathbf{x} \rangle_{\mathbf{K}}}$. The norm of a matrix $\mathbf{X} \in \mathbb{R}^{N \times M}$ induced by the vector norm $\|\cdot\|_{\mathbf{K}}$ is defined as $\|\mathbf{X}\|_{\mathbf{K}} := \max_{\mathbf{y} \neq \mathbf{0}} \|\mathbf{X}\mathbf{y}\|_{\mathbf{K}} / \|\mathbf{y}\|_{\mathbf{K}}$, and note that $\|\mathbf{X}\mathbf{y}\|_{\mathbf{K}} \leq \|\mathbf{X}\|_{\mathbf{K}} \|\mathbf{y}\|_{\mathbf{K}}$ for any vector $\mathbf{y} \in \mathbb{R}^M$. The spectral norm of a matrix is denoted as $\|\mathbf{X}\|_2$ when we choose $\mathbf{K} = \mathbf{I}_M$ as the $M \times M$ identity matrix [43].

A set $C \subset \mathbb{R}^M$ is said to be convex if $\alpha \mathbf{x} + (1 - \alpha) \mathbf{y} \in C$, $\forall \mathbf{x}, \mathbf{y} \in C$, $\forall \alpha \in (0, 1)$. If in addition the set C is closed, we call it a closed convex set. The \mathbf{K} -projection of a vector $\mathbf{w} \in \mathbb{R}^M$ onto a closed convex set C is denoted by $P_C^{\mathbf{K}}(\mathbf{w})$ which is the vector satisfying $\|\mathbf{w} - P_C^{\mathbf{K}}(\mathbf{w})\|_{\mathbf{K}} = \min_{\mathbf{v} \in C} \|\mathbf{w} - \mathbf{v}\|_{\mathbf{K}} =: d_{\mathbf{K}}(\mathbf{w}, C)$ [44], [45]. A vector $\Theta'(\mathbf{y}) \in \mathbb{R}^M$ is a subgradient of a function $\Theta : \mathbb{R}^M \rightarrow \mathbb{R}$ at $\mathbf{y} \in \mathbb{R}^M$ if $\Theta(\mathbf{y}) + \langle \mathbf{x} - \mathbf{y}, \Theta'(\mathbf{y}) \rangle \leq \Theta(\mathbf{x})$ for all $\mathbf{x} \in \mathbb{R}^M$. The c -level set of the function Θ is defined by $\text{lev}_{\leq c} \Theta := \{\mathbf{w} \in \mathbb{R}^M \mid \Theta(\mathbf{w}) \leq c\}$, $c \in \mathbb{R}$. If $\Theta : \mathbb{R}^M \rightarrow \mathbb{R}$ is convex $\text{lev}_{\leq c} \Theta$ is a closed convex set for every $c \in \mathbb{R}$ [46].

B. System Model

We address the problem of distributed adaptive learning of a continuous, nonlinear function (or system) $\psi : \mathcal{X} \rightarrow \mathbb{R}$ by a network of J nodes where $\mathcal{X} \subseteq \mathbb{R}^L$ is the input space and \mathbb{R} the output space. We label a node by index j and the time by index k . Each node j observes the unknown, nonlinear function ψ by sequentially feeding it with inputs $\mathbf{x}_{j,k} \in \mathbb{R}^L$. Thus, each node j acquires the measurement $d_{j,k} \in \mathbb{R}$ per time index k via

$$d_{j,k} = \psi(\mathbf{x}_{j,k}) + n_{j,k}, \quad (1)$$

where $n_{j,k} \in \mathbb{R}$ is a noise sample. Based on the nodes' observations, at each time index k we have a set of J acquired input-output samples $\{(\mathbf{x}_{j,k}, d_{j,k})\}_{j \in \mathcal{J}}$ available within the network.

To describe the connections among the nodes in the network we employ a graph $\mathcal{G} = (\mathcal{J}, \mathcal{E})$ with a set of nodes $\mathcal{J} = \{1, \dots, J\}$ and a set of edges $\mathcal{E} \subseteq \mathcal{J} \times \mathcal{J}$. Each edge in the network represents a connection between two nodes j and i given by $(j, i) \in \mathcal{E}$ where each node j is connected to itself, i.e., $(j, j) \in \mathcal{E}$. We further assume that the graph is *undirected*, i.e., edges (j, i) and (i, j) are equivalent to each other. The set of neighbors for each node j is given as $\mathcal{N}_j = \{i \in \mathcal{J} \mid (j, i) \in \mathcal{E}\}$ containing all nodes connected to node j (including node j itself). Furthermore, we consider the graph to be *connected*, i.e., each node can be reached by any other node over multiple hops. The objective of the nodes is to learn the nonlinear function ψ based on the acquired input-output samples $\{(\mathbf{x}_{j,k}, d_{j,k})\}_{j \in \mathcal{J}}$ in a distributed fashion. To this end, nodes are able to exchange information with their neighboring nodes to enhance their individual estimate of the unknown function ψ .

C. Multikernel Adaptive Filter

For the approximation of ψ we employ a multikernel adaptive filter and model the function by multiple positive definite kernels $\kappa_q : \mathcal{X} \times \mathcal{X} \rightarrow \mathbb{R}$ with $q \in \mathcal{Q} = \{1, 2, \dots, Q\}$ [31]. Each kernel κ_q induces an RKHS \mathcal{H}_q [13], and the multikernel adaptive filter uses corresponding dictionaries $\mathcal{D}_q = \{\kappa_q(\cdot, \bar{\mathbf{x}}_\ell)\}_{\ell=1}^r$, each of cardinality r . Here, each dictionary \mathcal{D}_q contains kernel functions κ_q centered at samples $\bar{\mathbf{x}}_\ell \in \mathcal{X}$ which are used to approximate ψ . For simplicity, we assume that each dictionary \mathcal{D}_q uses the same centers $\{\bar{\mathbf{x}}_\ell\}_{\ell=1}^r$ although this assumption is unnecessary. The multikernel adaptive filter $\varphi : \mathcal{X} \rightarrow \mathbb{R}$ is then given by

$$\varphi(\cdot) = \sum_{q \in \mathcal{Q}} \sum_{\ell=1}^r w_{q,\ell} \kappa_q(\cdot, \bar{\mathbf{x}}_\ell) \quad (2a)$$

$$= \sum_{q \in \mathcal{Q}} \varphi_{(q)}(\cdot), \quad (2b)$$

where $\varphi_{(q)}(\cdot) = \sum_{\ell=1}^r w_{q,\ell} \kappa_q(\cdot, \bar{\mathbf{x}}_\ell)$. With the above formulation we can compute the output of the function φ for

arbitrary input samples \mathbf{x} via

$$\varphi(\mathbf{x}) = \sum_{q \in \mathcal{Q}} \varphi_{(q)}(\mathbf{x}) = \sum_{q \in \mathcal{Q}} \langle \varphi_{(q)}, \kappa_q(\cdot, \mathbf{x}) \rangle_{\mathcal{H}_q} \quad (3a)$$

$$= \sum_{q \in \mathcal{Q}} \sum_{\ell=1}^r w_{q,\ell} \kappa_q(\mathbf{x}, \bar{\mathbf{x}}_\ell) \quad (3b)$$

$$= \langle \mathbf{w}, \boldsymbol{\kappa}(\mathbf{x}) \rangle_{\mathbb{R}^{rQ}}, \quad (3c)$$

due to the *reproducing property* $\varphi_{(q)}(\mathbf{x}) = \langle \varphi_{(q)}, \kappa_q(\cdot, \mathbf{x}) \rangle_{\mathcal{H}_q}$ of a kernel in its RKHS [13]. Here, vectors \mathbf{w} and $\boldsymbol{\kappa}(\mathbf{x})$ are defined as

$$\begin{aligned} \mathbf{w}_{(q)} &:= [w_{q,1}, \dots, w_{q,r}]^\top \in \mathbb{R}^r, \\ \mathbf{w} &:= [\mathbf{w}_{(1)}^\top, \dots, \mathbf{w}_{(Q)}^\top]^\top \in \mathbb{R}^{rQ}, \\ \boldsymbol{\kappa}_q(\mathbf{x}) &:= [\kappa_q(\mathbf{x}, \bar{\mathbf{x}}_1), \dots, \kappa_q(\mathbf{x}, \bar{\mathbf{x}}_r)]^\top \in \mathbb{R}^r, \\ \boldsymbol{\kappa}(\mathbf{x}) &:= [\boldsymbol{\kappa}_1^\top(\mathbf{x}), \dots, \boldsymbol{\kappa}_Q^\top(\mathbf{x})]^\top \in \mathbb{R}^{rQ}. \end{aligned}$$

A commonly used kernel function is the Gaussian kernel defined as

$$\kappa_q(\mathbf{x}_1, \mathbf{x}_2) := \exp\left(-\frac{\|\mathbf{x}_1 - \mathbf{x}_2\|_{\mathbb{R}^L}^2}{2\zeta_q^2}\right), \quad \mathbf{x}_1, \mathbf{x}_2 \in \mathcal{X}, \quad (4)$$

where $\zeta_q > 0$ is the kernel bandwidth. The metric of an RKHS is determined by the kernel Gram matrix. It contains the inherent correlations of a dictionary \mathcal{D}_q with respect to (w.r.t.) the kernel κ_q and is defined as

$$\mathbf{K}_q := \begin{bmatrix} \kappa_q(\bar{\mathbf{x}}_1, \bar{\mathbf{x}}_1) & \dots & \kappa_q(\bar{\mathbf{x}}_1, \bar{\mathbf{x}}_r) \\ \vdots & \ddots & \vdots \\ \kappa_q(\bar{\mathbf{x}}_r, \bar{\mathbf{x}}_1) & \dots & \kappa_q(\bar{\mathbf{x}}_r, \bar{\mathbf{x}}_r) \end{bmatrix} \in \mathbb{R}^{r \times r}. \quad (5)$$

Assuming that each dictionary \mathcal{D}_q is linearly independent it follows that each \mathbf{K}_q is positive-definite [45]. Moreover, we introduce the multikernel Gram matrix $\mathbf{K} := \text{blkdiag}\{\mathbf{K}_1, \mathbf{K}_2, \dots, \mathbf{K}_Q\} \in \mathbb{R}^{rQ \times rQ}$ being the block-diagonal matrix of the Gram matrices of all kernels. Then, by virtue of Lemma 1 from [47] we can parameterize φ by \mathbf{w} in the Euclidean space \mathbb{R}^{rQ} using the \mathbf{K} inner product $\langle \cdot, \cdot \rangle_{\mathbf{K}}$. The \mathbf{K} -metric in the Euclidean space corresponds to the metric of the Cartesian product of multiple RKHSs [32]. Indeed, we can express (3c) equivalently by

$$\varphi(\mathbf{x}) = \langle \mathbf{w}, \boldsymbol{\kappa}(\mathbf{x}) \rangle_{\mathbb{R}^{rQ}} = \langle \mathbf{w}, \mathbf{K}^{-1} \boldsymbol{\kappa}(\mathbf{x}) \rangle_{\mathbf{K}}. \quad (6)$$

Instead of applying a learning method to the function φ in $(\mathcal{H}, \langle \cdot, \cdot \rangle_{\mathcal{H}})$ we can directly apply it to the coefficient vector $\mathbf{w} \in \mathbb{R}^{rQ}$ in $(\mathbb{R}^{rQ}, \langle \cdot, \cdot \rangle_{\mathbf{K}})$. This representation is based on the *parameter-space approach* from the kernel adaptive filtering literature with the *functional-space approach* as its equivalent counterpart, see [31, Appendix A].

D. Problem Formulation

Based on the parametrization of the estimator φ by the coefficient vector \mathbf{w} we are now able to formulate an optimization problem on \mathbf{w} . The objective is to find a \mathbf{w} such that the estimated output $\varphi(\mathbf{x}) = \langle \mathbf{w}, \mathbf{K}^{-1} \boldsymbol{\kappa}(\mathbf{x}) \rangle_{\mathbf{K}}$ is close to the function output $\psi(\mathbf{x})$ for arbitrary input samples $\mathbf{x} \in \mathcal{X}$. This has to be achieved in a distributed fashion for each node j in the network based on the acquired input-output

samples $\{(\mathbf{x}_{j,k}, d_{j,k})\}_{j \in \mathcal{J}}$. Thus, we equip each node j with a multikernel adaptive filter φ_j parametrized by its individual coefficient vector \mathbf{w}_j . Furthermore, each node j is assumed to rely on the same dictionaries $\mathcal{D}_q, q \in \mathcal{Q}$, i.e., they are globally known and common to all nodes. To specify the coefficient vectors which result in an estimate close to the node's measurement, we introduce the closed convex set $\mathcal{S}_{j,k}$ per node j and time index k :

$$\mathcal{S}_{j,k} := \{\mathbf{w}_j \in \mathbb{R}^{rQ} : |\langle \mathbf{w}_j, \mathbf{K}^{-1} \boldsymbol{\kappa}(\mathbf{x}_{j,k}) \rangle_{\mathbf{K}} - d_{j,k}| \leq \varepsilon_j\},$$

where $\varepsilon_j \geq 0$ is a design parameter. The set $\mathcal{S}_{j,k}$ is a *hyperslab* containing those vectors \mathbf{w}_j which provide an estimate $\varphi(\mathbf{x}_{j,k})$ with a maximum distance of ε_j to the desired output $d_{j,k}$ [48]. The parameter ε_j controls the thickness of the hyperslab $\mathcal{S}_{j,k}$, and is introduced to consider the uncertainty caused by measurement noise $n_{j,k}$. The key issue is to find an optimal $\mathbf{w}_j \in \mathcal{S}_{j,k}$. To this end, we define a local cost function $\Theta_{j,k}$ at time k per node j as the metric distance between its coefficient vector \mathbf{w}_j and the hyperslab $\mathcal{S}_{j,k}$ in the \mathbf{K} -norm sense:

$$\Theta_{j,k}(\mathbf{w}_j) := d_{\mathbf{K}}(\mathbf{w}_j, \mathcal{S}_{j,k}) = \|\mathbf{w}_j - P_{\mathcal{S}_{j,k}}^{\mathbf{K}}(\mathbf{w}_j)\|_{\mathbf{K}}. \quad (7)$$

This cost function gives the residual between \mathbf{w}_j and its \mathbf{K} -projection onto $\mathcal{S}_{j,k}$. It has been shown that using the \mathbf{K} -norm delivers faster convergence compared to the usual Euclidean metric [23]. Using the APSM framework such a cost function leads in its core to the kernel normalized least-squares (KNLMS) algorithm but with a modified metric [27]. We aim at minimizing the global cost functions $\Theta_k(\mathbf{w}_j) := \sum_{j \in \mathcal{J}} \Theta_{j,k}(\mathbf{w}_j)$ over time k at all nodes in the network where each individual cost $\Theta_{j,k}$ is time-varying. Simultaneously, we require all coefficient vectors \mathbf{w}_j to converge to the same solution, which guarantees consensus in the network on the individual estimates \mathbf{w}_j . Thus, the objective is to minimize the sequence $(\Theta_k)_{k \in \mathbb{N}}$ of global cost functions. To this end, we consider the following optimization problem at time k as in [8], [10], [49]:

$$\min_{\{\mathbf{w}_j | j \in \mathcal{J}\}} \sum_{j \in \mathcal{J}} \Theta_{j,k}(\mathbf{w}_j) \quad (8a)$$

$$\text{s.t. } \mathbf{w}_j = \mathbf{w}_i, \quad \forall i \in \mathcal{N}_j. \quad (8b)$$

Constraint (8b) enforces all coefficient vectors to converge to the same solution, i.e., $\mathbf{w}_1 = \mathbf{w}_2 = \dots = \mathbf{w}_J$ guaranteeing consensus within the network.

With regard to problem (8) let us define the optimal solution set as

$$\Upsilon^* := \bigcap_{k \geq 0} \bigcap_{j \in \mathcal{J}} \Upsilon_{j,k}, \quad (9)$$

where $\Upsilon_{j,k} := \arg \min_{\mathbf{w}_j \in \mathbb{R}^{rQ}} \Theta_{j,k}(\mathbf{w}_j)$. Then the set Υ^* contains those points which minimize $\Theta_{j,k}$ for all nodes $j \in \mathcal{J}$ and at every time instant $k \in \mathbb{N}$ under the assumption that Υ^* is nonempty. Therefore, a vector $\mathbf{w}^* \in \Upsilon^*$ is called *ideal estimate*. Finding $\mathbf{w}^* \in \Upsilon^*$ is a challenging task particularly under practical considerations. Due to limited memory, for instance, not all measurements can be stored over time at each node. Hence, information about the set Υ^* is unavailable and

thus an ideal estimate \mathbf{w}^* cannot be acquired. An alternative, feasible task is the minimization of all but finitely many global costs Θ_k . This approach stems from the intuition that a good estimate should minimize as many costs Θ_k as possible. To acquire such an estimate the nodes should agree on a point contained in the following set:

$$\Upsilon := \overline{\liminf_{k \rightarrow \infty} \Upsilon_k} = \bigcup_{k=0}^{\infty} \bigcap_{m \geq k} \Upsilon_m \supset \Upsilon^* \quad (10)$$

where $\Upsilon_k := \bigcap_{j \in \mathcal{J}} \Upsilon_{j,k}$ and the overbar gives the closure of a set. Finding a point in the set Υ is clearly a less restrictive task than finding one in Υ^* since all global costs Θ_k excluding finitely many ones need to be minimized. Therefore, our proposed algorithm should achieve estimates contained in the set Υ .

III. PROPOSED ALGORITHM: DIFFUSION-BASED MULTIKERNEL ADAPTIVE FILTER

To solve (8) in a distributed way we employ a two-step scheme consisting of a local adaptation and a diffusion stage which has been commonly used in the literature, see e.g. [4], [35], [49]:

- 1) a *local APSM update* per node j on the coefficient vector \mathbf{w}_j giving an intermediate coefficient vector \mathbf{w}'_j ;
- 2) a *diffusion stage* to fuse vectors \mathbf{w}'_i from neighboring nodes $i \in \mathcal{N}_j$ to update \mathbf{w}_j .

Step 1) ensures that each local cost $\Theta_{j,k}$ is reduced, and, hence the global cost $\Theta_k = \sum_{j \in \mathcal{J}} \Theta_{j,k}$ is reduced as well. Step 2) seeks for a consensus among all coefficient vectors $\{\mathbf{w}_j\}_{j \in \mathcal{J}}$ in order to satisfy constraint (8b).

A. Local APSM Update

The APSM asymptotically minimizes a sequence of nonnegative convex (not necessarily differentiable) functions [27] and can thus be used to minimize the local cost function $\Theta_{j,k}(\mathbf{w}_j)$ in (7) per node j . For the coefficient vector $\mathbf{w}_{j,k} \in \mathbb{R}^{rQ}$ at node j and time k a particular case of the APSM update with the \mathbf{K} -norm reads

$$\mathbf{w}'_{j,k+1} := \mathbf{w}_{j,k} - \mu_{j,k} \frac{\Theta_{j,k}(\mathbf{w}_{j,k}) - \Theta_{j,k}^*(\mathbf{w}_j)}{\|\Theta'_{j,k}(\mathbf{w}_{j,k})\|_{\mathbf{K}}^2} \Theta'_{j,k}(\mathbf{w}_{j,k}) \quad (11)$$

if $\Theta'_{j,k}(\mathbf{w}_{j,k}) \neq \mathbf{0}$. Otherwise, no update is conducted such that $\mathbf{w}'_{j,k+1} := \mathbf{w}_{j,k}$. Here, $\Theta_{j,k}^* := \min_{\mathbf{w}_j} \Theta_{j,k}(\mathbf{w}_j)$ and for (7) we have $\Theta_{j,k}^* = 0$. The parameter $\mu_{j,k} \in (0, 2)$ is the step size. Since the cost function $\Theta_{j,k}$ measures the distance w.r.t. the \mathbf{K} -norm we need to use the \mathbf{K} -metric for the squared norm in the denominator. A subgradient for (7) is given by [27]

$$\Theta'_{j,k}(\mathbf{w}_{j,k}) = \frac{\mathbf{w}_{j,k} - P_{\mathcal{S}_{j,k}}^{\mathbf{K}}(\mathbf{w}_{j,k})}{\|\mathbf{w}_{j,k} - P_{\mathcal{S}_{j,k}}^{\mathbf{K}}(\mathbf{w}_{j,k})\|_{\mathbf{K}}}, \quad \text{for } \mathbf{w}_{j,k} \notin \mathcal{S}_{j,k}. \quad (12)$$

For this subgradient we have $\|\Theta'_{j,k}(\mathbf{w}_{j,k})\|_{\mathbf{K}}^2 = 1$ and thus we arrive at the following APSM update per node j :

$$\mathbf{w}'_{j,k+1} := \mathbf{w}_{j,k} - \mu_{j,k} \left(\mathbf{w}_{j,k} - P_{\mathcal{S}_{j,k}}^{\mathbf{K}}(\mathbf{w}_{j,k}) \right). \quad (13)$$

As we can see, the difference vector $\mathbf{w}_{j,k} - P_{\mathcal{S}_{j,k}}^{\mathbf{K}}(\mathbf{w}_{j,k})$ is used to move the coefficient vector $\mathbf{w}_{j,k}$ into the direction of the hyperslab $\mathcal{S}_{j,k}$ controlled by the step size $\mu_{j,k}$. Note that this update solely relies on local information, i.e., no information from neighboring nodes is needed. The projection $P_{\mathcal{S}_{j,k}}^{\mathbf{K}}(\mathbf{w}_{j,k})$ can be calculated by [44]

$$P_{\mathcal{S}_{j,k}}^{\mathbf{K}}(\mathbf{w}) = \begin{cases} \mathbf{w}, & \text{if } \mathbf{w} \in \mathcal{S}_{j,k} \\ \mathbf{w} - \frac{\mathbf{w}^{\top} \boldsymbol{\kappa}(\mathbf{x}_{j,k}) - d_{j,k} - \varepsilon_j}{\|\mathbf{K}^{-1} \boldsymbol{\kappa}(\mathbf{x}_{j,k})\|_{\mathbf{K}}^2} \mathbf{K}^{-1} \boldsymbol{\kappa}(\mathbf{x}_{j,k}), & \text{if } \mathbf{w}^{\top} \boldsymbol{\kappa}(\mathbf{x}_{j,k}) > d_{j,k} + \varepsilon_j \\ \mathbf{w} - \frac{\mathbf{w}^{\top} \boldsymbol{\kappa}(\mathbf{x}_{j,k}) - d_{j,k} + \varepsilon_j}{\|\mathbf{K}^{-1} \boldsymbol{\kappa}(\mathbf{x}_{j,k})\|_{\mathbf{K}}^2} \mathbf{K}^{-1} \boldsymbol{\kappa}(\mathbf{x}_{j,k}), & \text{if } \mathbf{w}^{\top} \boldsymbol{\kappa}(\mathbf{x}_{j,k}) < d_{j,k} - \varepsilon_j. \end{cases} \quad (14)$$

B. Diffusion Stage

To satisfy constraint (8b) and to reach consensus on the coefficient vectors \mathbf{w}_j , each node j fuses its own vector \mathbf{w}'_j with those of its neighbors $\{\mathbf{w}'_i\}_{i \in \mathcal{N}_j}$. To this end, we employ a symmetric matrix $\mathbf{G} \in \mathbb{R}^{J \times J}$ assigning weights to the edges in the network. The (j, i) -entry of \mathbf{G} is denoted by g_{ji} and gives the weight on the edge between nodes j and i . Obviously, if no connection is present among both nodes, the entry will be zero. The fusion per node j at time k follows

$$\mathbf{w}_{j,k} := \sum_{i \in \mathcal{N}_j} g_{ji} \mathbf{w}'_{i,k}. \quad (15)$$

To guarantee that all nodes converge to the same coefficient vector, \mathbf{G} needs to fulfill the following conditions [10]:

$$\|\mathbf{G} - (1/J) \mathbf{1}_J \mathbf{1}_J^{\top}\|_2 < 1, \quad \mathbf{G} \mathbf{1}_J = \mathbf{1}_J, \quad (16)$$

where $\mathbf{1}_J$ is the vector of J ones. The first condition guarantees convergence to the average of all states in the network while the second condition keeps the network at a stable state if consensus has been reached. Such matrices have been vastly applied in literature for consensus averaging problems, see e.g. [4], [50], [51]. Our proposed algorithm to solve (8) is then given by the following update equations per node j and time index k :

$$\mathbf{w}'_{j,k+1} := \mathbf{w}_{j,k} - \mu_{j,k} \left(\mathbf{w}_{j,k} - P_{\mathcal{S}_{j,k}}^{\mathbf{K}}(\mathbf{w}_{j,k}) \right) \quad (17a)$$

$$\mathbf{w}_{j,k+1} := \sum_{i \in \mathcal{N}_j} g_{ji} \mathbf{w}'_{i,k+1} \quad (17b)$$

where the projection $P_{\mathcal{S}_{j,k}}^{\mathbf{K}}(\mathbf{w}_{j,k})$ is given in (14). In each iteration k each node j performs a local APSM update and transmits its intermediate coefficient vector $\mathbf{w}'_{j,k}$ to its neighbors $i \in \mathcal{N}_j$. After receiving the intermediate coefficient vectors $\mathbf{w}'_{i,k}$ from their neighbors, each node fuses these with its own vector $\mathbf{w}'_{j,k}$ by a weighted average step.

In factor, (17a) comprises the projection in the Cartesian product of Q RKHSs which is used by the CHYPASS algorithm from [32]. Therefore, we call our proposed scheme the diffusion-based Cartesian hyperplane projection along affine subspace (D-CHYPASS) algorithm being a distributed implementation of CHYPASS.

IV. THEORETICAL PROPERTIES

A. Consensus Matrix

To analyze the theoretical properties of the D-CHYPASS algorithm, let us first introduce the definition of the consensus matrix.

Definition 1 (Consensus Matrix [10]): A consensus matrix $\mathbf{P} \in \mathbb{R}^{rQJ \times rQJ}$ is a square matrix satisfying the following two properties.

- 1) $\mathbf{P}\mathbf{z} = \mathbf{z}$ and $\mathbf{P}^\top \mathbf{z} = \mathbf{z}$ for any vector $\mathbf{z} \in \mathcal{C} := \{\mathbf{1}_J \otimes \mathbf{a} \in \mathbb{R}^{rQJ} \mid \mathbf{a} \in \mathbb{R}^{rQ}\}$.
- 2) The rQ largest singular values of \mathbf{P} are equal to one and the remaining $rQJ - rQ$ singular values are strictly less than one.

We denote by \otimes the Kronecker product. We can further establish the following properties of the consensus matrix \mathbf{P} :

Lemma 1 (Properties of Consensus Matrix [10]): Let $\mathbf{e}_n \in \mathbb{R}^{rQ}$ be a unit vector with its n -th entry being one and $\mathbf{b}_n = (\mathbf{1}_J \otimes \mathbf{e}_n) / \sqrt{J} \in \mathbb{R}^{rQJ}$. Further, we define the consensus subspace $\mathcal{C} := \text{span}\{\mathbf{b}_1, \dots, \mathbf{b}_{rQ}\}$ and the stacked vector of all coefficient vectors in the network $\mathbf{z}_k = [\mathbf{w}_{1,k}^\top, \dots, \mathbf{w}_{J,k}^\top]^\top \in \mathbb{R}^{rQJ}$. Then, we have the following properties.

- 1) The consensus matrix \mathbf{P} can be decomposed into $\mathbf{P} = \mathbf{B}\mathbf{B}^\top + \mathbf{X}$ with $\mathbf{B} := [\mathbf{b}_1 \dots \mathbf{b}_{rQ}] \in \mathbb{R}^{rQJ \times rQ}$ and $\mathbf{X} \in \mathbb{R}^{rQJ \times rQJ}$ satisfying $\mathbf{X}\mathbf{B}\mathbf{B}^\top = \mathbf{B}\mathbf{B}^\top \mathbf{X} = \mathbf{0}$ and $\|\mathbf{X}\|_2 < 1$.
- 2) The nodes have reached consensus at time index k if and only if $(\mathbf{I}_{rQJ} - \mathbf{B}\mathbf{B}^\top)\mathbf{z}_k = \mathbf{0}$, i.e., $\mathbf{z}_k \in \mathcal{C}$.

A consensus matrix can be constructed by matrix \mathbf{G} as $\mathbf{P} = \mathbf{G} \otimes \mathbf{I}_{rQ}$ where \mathbf{I}_{rQ} is the $rQ \times rQ$ identity matrix. The matrix \mathbf{P} is then said to be compatible to the graph \mathcal{G} since $\mathbf{z}_{k+1} = \mathbf{P}\mathbf{z}_k$ can be equivalently calculated by $\mathbf{w}_{j,k+1} = \sum_{i \in \mathcal{N}_j} g_{ji} \mathbf{w}_{i,k}$ (see (15)) [10]. By definition of the consensus matrix we know that $\|\mathbf{P}\|_2 = 1$ holds. However, for further analysis of the D-CHYPASS algorithm, we need to know the norm w.r.t. matrix \mathbf{K} since D-CHYPASS uses the \mathbf{K} -metric. Therefore, we introduce a modified consensus matrix $\hat{\mathbf{P}}$ satisfying $\|\hat{\mathbf{P}}\|_{\mathcal{K}} = 1$.

Lemma 2 (Modified Consensus Matrix): Suppose that \mathbf{P} is a consensus matrix defined as in Definition 1. Let

$$\hat{\mathbf{P}} := \mathcal{K}^{-1/2} \mathbf{P} \mathcal{K}^{1/2}$$

be the modified consensus matrix where \mathcal{K} is the block-diagonal matrix with J copies of \mathbf{K} :

$$\mathcal{K} := \mathbf{I}_J \otimes \mathbf{K} \in \mathbb{R}^{rQJ \times rQJ}. \quad (18)$$

Assume further, that the dictionary $\mathcal{D}_q = \{\kappa_q(\cdot, \bar{\mathbf{x}}_\ell)\}_{\ell=1}^r$ for each $q \in \mathcal{Q}$ is linearly independent, i.e., its corresponding kernel Gram matrix \mathbf{K}_q is of full rank, and thus \mathcal{K} is also linearly independent. Then, the \mathcal{K} -norm of $\hat{\mathbf{P}}$ is given by $\|\hat{\mathbf{P}}\|_{\mathcal{K}} = 1$. In particular, it holds that both consensus matrices are equivalent to each other, $\hat{\mathbf{P}} = \mathbf{P}$.

Proof: The proof is given in Appendix A. \blacksquare

Due to Lemma 2, for further analysis we are free to use either \mathbf{P} or $\hat{\mathbf{P}}$ and it holds that $\|\mathbf{P}\|_{\mathcal{K}} = \|\hat{\mathbf{P}}\|_{\mathcal{K}} = 1$.

B. Convergence Analysis

Examining (17) we can summarize both update equations of the D-CHYPASS in terms of all coefficient vectors in the network by defining

$$\mathbf{z}_k := \begin{bmatrix} \mathbf{w}_{1,k} \\ \vdots \\ \mathbf{w}_{J,k} \end{bmatrix}, \quad \Phi_k := \begin{bmatrix} \mu_{j,k}(\mathbf{w}_{1,k} - P_{S_{1,k}}(\mathbf{w}_{1,k})) \\ \vdots \\ \mu_{j,k}(\mathbf{w}_{J,k} - P_{S_{J,k}}(\mathbf{w}_{J,k})) \end{bmatrix}$$

and rewriting (17a) and (17b) into

$$\mathbf{z}_{k+1} = (\mathbf{G} \otimes \mathbf{I}_{rQ})(\mathbf{z}_k - \Phi_k). \quad (19)$$

In the following, we show the convergence properties of D-CHYPASS for fixed and deterministic network topologies. Although the space under study is the \mathbf{K} -metric space unlike [8], [10] we can still prove the properties due to Lemmas 1 and 2.

Theorem 1: The sequence $(\mathbf{z}_k)_{k \in \mathbb{N}}$ generated by (19) satisfies the following.

- 1) *Monotone approximation:* Assume that $\mathbf{w}_{j,k} \notin \mathcal{S}_{j,k}$, $\mu_{j,k} \in (0, 2)$ for at least one node j and that $\mu_i \in [0, 2]$ ($i \neq j$). Then, for every $\mathbf{w}_k^* \in \Upsilon_k$ it holds that

$$\|\mathbf{z}_{k+1} - \mathbf{z}_k^*\|_{\mathcal{K}} < \|\mathbf{z}_k - \mathbf{z}_k^*\|_{\mathcal{K}} \quad (20)$$

with $\mathbf{z}_k^* := [(\mathbf{w}_k^*)^\top, (\mathbf{w}_k^*)^\top, \dots, (\mathbf{w}_k^*)^\top]^\top \in \mathbb{R}^{rQJ}$.

For the remaining properties we assume that $\mu_{j,k} \in [\epsilon_1, 2 - \epsilon_2]$ with $\epsilon_1, \epsilon_2 > 0$ and $\mathbf{w}^* \in \Upsilon^* \neq \emptyset$. We further define $\mathbf{z}^* := [(\mathbf{w}^*)^\top, (\mathbf{w}^*)^\top, \dots, (\mathbf{w}^*)^\top]^\top$. Then the following holds:

- 2) *Asymptotic minimization of local costs:* For every \mathbf{z}^* the local costs $\Theta_{j,k}(\mathbf{w}_{j,k}) = \|\mathbf{w}_{j,k} - P_{S_{j,k}}(\mathbf{w}_{j,k})\|_{\mathcal{K}}$ are asymptotically minimized, i.e.,

$$\lim_{k \rightarrow \infty} \Theta_{j,k}(\mathbf{w}_{j,k}) = 0, \quad \forall j \in \mathcal{J}. \quad (21)$$

- 3) *Asymptotic consensus:* With the decomposition $\mathbf{P} = \mathbf{B}\mathbf{B}^\top + \mathbf{X}$ and $\|\mathbf{X}\|_2 < 1$ the sequence $(\mathbf{z}_k)_{k \in \mathbb{N}}$ asymptotically achieves consensus such that

$$\lim_{k \rightarrow \infty} (\mathbf{I}_{rQJ} - \mathbf{B}\mathbf{B}^\top)\mathbf{z}_k = \mathbf{0}. \quad (22)$$

- 4) *Convergence of $(\mathbf{z}_k)_{k \in \mathbb{N}}$:* Suppose that Υ^* has a nonempty interior, i.e., there exists $\rho > 0$ and interior point $\tilde{\mathbf{u}}$ such that $\{\mathbf{v} \in \mathbb{R}^{rQ} \mid \|\mathbf{v} - \tilde{\mathbf{u}}\|_{\mathcal{K}} \leq \rho\} \subset \Upsilon^*$. Then, the sequence $(\mathbf{z}_k)_{k \in \mathbb{N}}$ converges to a vector $\hat{\mathbf{z}} = [\hat{\mathbf{w}}^\top, \dots, \hat{\mathbf{w}}^\top]^\top \in \mathcal{C}$ satisfying $(\mathbf{I}_{rQJ} - \mathbf{B}\mathbf{B}^\top)\hat{\mathbf{z}} = \mathbf{0}$.

- 5) *Characterization of limit point $\hat{\mathbf{z}}$:* Suppose for an interior $\tilde{\mathbf{u}} \in \Upsilon^*$ that for any $\epsilon > 0$ and any $\eta > 0$ there exists a $\zeta > 0$ such that

$$\min_{k \in \mathcal{I}} \sum_{j \in \mathcal{J}} \|\mathbf{w}_{j,k} - P_{S_{j,k}}(\mathbf{w}_{j,k})\|_{\mathcal{K}} \geq \zeta, \quad (23)$$

where

$$\mathcal{I} := \left\{ k \in \mathbb{N} \mid \sum_{j \in \mathcal{J}} d_{\mathbf{K}}(\mathbf{w}_{j,k}, \text{lev}_{\leq 0} \Theta_{j,k}) > \epsilon \right.$$

$$\left. \text{and } \sum_{j \in \mathcal{J}} \|\tilde{\mathbf{u}} - \mathbf{w}_{j,k}\|_{\mathcal{K}} \leq \eta \right\}.$$

Then it holds that $\hat{\mathbf{w}} \in \Upsilon$ with Υ defined as in (10).

Proof: The proof is given in Appendix B. \blacksquare

V. NUMERICAL EXAMPLES

In the following section, we evaluate the performance of the D-CHYPASS by applying it to the spatial reconstruction of multiple Gaussian functions, real altitude data and the tracking of a time-varying nonlinear function by a network of nodes. The nodes are distributed over the unit-square area A and each node j uses its Cartesian position vector $\mathbf{x}_j = [x_{j,1}, x_{j,2}]^\top \in \mathcal{X}$ as its regressor. We assume that the positions of the nodes stay fixed, i.e., $\mathbf{x}_{j,k}$ does not change over time. This is not necessary for the D-CHYPASS to be applicable, e.g. it can be applied to a mobile network where the positions change over time. Per time index k the nodes take a new measurement $d_{j,k}$ of the function ψ at their position \mathbf{x}_j . Hence, the network constantly monitors the function ψ . For all experiments we assume model (1) with zero-mean white Gaussian noise of variance σ_n^2 .

We compare the performance of the D-CHYPASS to the RFF-DKLMS [36], the FATC-KLMS [35] and the multikernel distributed consensus-based estimation (MKDiCE) [34] which are state of the art algorithms for distributed kernel-based estimation. Both RFF-DKLMS and FATC-KLMS are single kernel approaches based on a diffusion mechanism. Assuming that the FATC-KLMS only considers local data in its adaptation step, both schemes exhibit the same number of transmissions per node as the D-CHYPASS. To enable a fair comparison we restrict the adaptation step of the FATC-KLMS to use local data only and extend the algorithm by multiple kernels as in D-CHYPASS. We call this scheme the diffusion-based multikernel least-mean-squares (DMKLMS). Its update equation per node j is given by

$$\mathbf{w}'_{j,k+1} := \mathbf{w}_{j,k} + \mu_{j,k} (d_{j,k} - \mathbf{w}_{j,k}^\top \boldsymbol{\kappa}(\mathbf{x}_{j,k})) \boldsymbol{\kappa}(\mathbf{x}_{j,k}) \quad (24a)$$

$$\mathbf{w}_{j,k+1} := \sum_{i \in \mathcal{N}_j} g_{ji} \mathbf{w}'_{i,k+1}. \quad (24b)$$

The RFF-DKLMS approximates kernel evaluations by random Fourier features such that no design of a specific dictionary set is necessary. However, its performance is highly dependent on the number of the utilized Fourier features which determines the dimension of the vectors to be exchanged. The MKDiCE is a distributed regression scheme based on kernel least squares with multiple kernels using the ADMM for its distributed mechanism. The number of transmissions per iteration is higher compared to the D-CHYPASS, RFF-DKLMS and DMKLMS. Naturally, it is not an adaptive filter but is included here for reference purposes. As benchmark performance, we consider the central CHYPASS algorithm given by

$$\mathbf{w}_{k+1} := \mathbf{w}_k - \mu \sum_{j \in \mathcal{J}} (\mathbf{w}_k - P_{\mathcal{S}_{j,k}}^{\mathbf{K}}(\mathbf{w}_k)). \quad (25)$$

The central CHYPASS requires all node positions and measurements $\{(\mathbf{x}_{j,k}, d_{j,k})\}_{j \in \mathcal{J}}$ per time index k at a single node to perform the projection $P_{\mathcal{S}_{j,k}}^{\mathbf{K}}(\mathbf{w}_k)$ onto each set $\mathcal{S}_{j,k}$.

Regarding the dictionaries we assume that each \mathcal{D}_q uses the same samples $\{\bar{\mathbf{x}}_\ell\}_{\ell=1}^r$. These samples are a subset of the node positions $\{\mathbf{x}_j\}_{j \in \mathcal{J}}$ in the network and are selected following the coherence criterion: A node position \mathbf{x}_j is compared to

every dictionary entry $\{\bar{\mathbf{x}}_\ell\}_{\ell=1}^r$ and is included as dictionary sample $\bar{\mathbf{x}}_{r+1}$ if it satisfies

$$\max_{q \in \mathcal{Q}} \max_{\ell=1, \dots, r} |\kappa_q(\mathbf{x}_j, \bar{\mathbf{x}}_\ell)| \leq \tau. \quad (26)$$

Here, $0 < \tau \leq 1$ is the coherence threshold controlling the cardinality of \mathcal{D}_q . The dictionary \mathcal{D}_q is generated a priori over all node positions before the algorithm iterates. After that it stays fixed throughout the reconstruction process for the specific algorithm.

As error metric we consider the network NMSE $_k$ per time k over the area A . It evaluates the normalized squared-difference between reconstructed field $\varphi_j(\mathbf{x})$ and the true field $\psi(\mathbf{x})$ averaged over all nodes:

$$\text{NMSE}_k := \frac{1}{J} \sum_{j \in \mathcal{J}} \frac{\mathbb{E} \left\{ \int_A |\psi(\mathbf{x}) - \mathbf{w}_{j,k}^\top \boldsymbol{\kappa}(\mathbf{x})|^2 d\mathbf{x} \right\}}{\int_A |\psi(\mathbf{x})|^2 d\mathbf{x}}. \quad (27)$$

The expectation in the numerator is approximated by averaging over independent trials. The integrals are approximated by a sum over regularly positioned grid points which sample the area A .

A. Multiple Gaussian Functions

As a first example we apply the D-CHYPASS algorithm to the reconstruction of two Gaussian functions with different bandwidths given as follows:

$$\psi(\mathbf{x}) := 2 \exp\left(-\frac{\|\mathbf{x} - \mathbf{p}_1\|_{\mathbb{R}^2}^2}{2 \cdot 0.1^2}\right) + \exp\left(-\frac{\|\mathbf{x} - \mathbf{p}_2\|_{\mathbb{R}^2}^2}{2 \cdot 0.3^2}\right)$$

with $\mathbf{p}_1 = [0.5, 0.7]^\top$, $\mathbf{p}_2 = [0.3, 0.1]^\top$, and the Cartesian coordinate vector $\mathbf{x} = [x_1, x_2]^\top$. We use $J = 60$ nodes randomly placed over $A = [0, 1]^2$ where nodes share a connection if their distance to each other satisfies $D < 0.3$. We assume a noise variance of $\sigma_n^2 = 0.3$ at the nodes and average the performance over 200 trials with a new network realization in each trial. Regarding the kernel choice we use two Gaussian kernels ($Q = 2$) with bandwidths $\zeta_1 = 0.1$ and $\zeta_2 = 0.3$. For all diffusion-based algorithms we use the Metropolis-Hastings weights [52] where each entry g_{ji} is determined by

$$g_{ji} = \begin{cases} \frac{1}{\max\{\delta_j, \delta_i\}} & \text{if } j \neq i \text{ and } (j, i) \in \mathcal{E} \\ 1 - \sum_{i \in \mathcal{N}_j \setminus \{j\}} \frac{1}{\max\{\delta_j, \delta_i\}} & \text{if } j = i \\ 0 & \text{otherwise} \end{cases}$$

and $\delta_j = |\mathcal{N}_j|$ denotes the degree of a node j . For all algorithms we set the coherence threshold τ such that the same average dictionary size of $\bar{r} = 33$ is utilized. Single kernel approaches use the arithmetic average of the bandwidths chosen for the multikernel schemes as their kernel bandwidth. We evaluate the D-CHYPASS (I) with a hyperplane projection, i.e., $\varepsilon_j = 0$, and the D-CHYPASS (II) with a hyperslab projection with $\varepsilon_j = 0.5$. The chosen parameter values for the considered algorithms are listed in Table I.

Figure 1 shows the NMSE over the iteration k . Both D-CHYPASS (I) and (II) significantly outperform the compared algorithms in terms of convergence speed and steady-state

TABLE I
PARAMETER VALUES FOR EXPERIMENT IN SECTION V-A

Algorithm	Parameters		
D-CHYPASS (I)	$\mu_{j,k} = 0.2$ $\varepsilon_j = 0$	$\tau = 0.95$	$\zeta_1 = 0.1$ $\zeta_2 = 0.3$
D-CHYPASS (II)	$\mu_{j,k} = 0.5$ $\varepsilon_j = 0.5$		
DMKLMS	$\mu_{j,k} = 0.1$		
MKDiCE	$\mu_{j,k} = 0.5$		
Central CHYPASS	$\mu = 3.3 \cdot 10^{-3}$ $\varepsilon_j = 0$		
FATC-KLMS	$\mu_{j,k} = 0.07$	$\tau = 0.9$	$\zeta = 0.2$
RFF-DKLMS (I)	$\mu_{j,k} = 0.1$	$r_{\text{RFF}} = 100$	
RFF-DKLMS (II)	$\mu_{j,k} = 0.1$	$r_{\text{RFF}} = 500$	

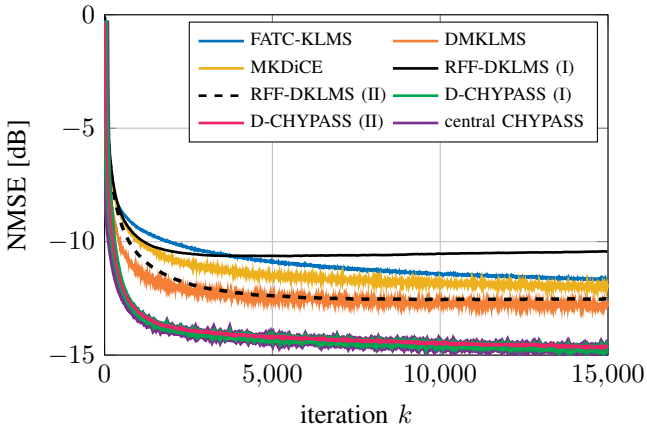


Fig. 1. Learning curves for the reconstruction of multiple Gaussian functions.

error. Regarding the single kernel approaches, FATC-KLMS outperforms RFF-DKLMS (I) in its steady-state error although it uses a dictionary of only $\bar{r} = 33$ samples compared to $r_{\text{RFF}} = 100$ random Fourier features. By increasing the number of Fourier features to $r_{\text{RFF}} = 500$ the performance can be significantly improved, cf. RFF-DKLMS (II). Nevertheless, this improvement comes with a huge increase in communication overhead since the number of Fourier features is equal to the dimension of the coefficient vectors to be exchanged. While DMKLMS exchanges vectors with $\bar{r}Q = 66$ entries only, the coefficient vectors in RFF-DKLMS (II) have $r_{\text{RFF}} = 500$ entries. Thus, by relying on an a priori designed dictionary as in DMKLMS and D-CHYPASS, huge savings in communication overhead and computational complexity can be achieved. The enhanced performance by D-CHYPASS compared to the other multikernel approaches is due to a better metric in form of the \mathbf{K} -norm and the normalization factor $\|\mathbf{K}^{-1}\kappa(\mathbf{x}_{j,k})\|_{\mathbf{K}}^2$ in the projection $P_{\mathcal{S}_{j,k}}(\mathbf{w}_{j,k})$ which adapts the step size $\mu_{j,k}$. By exploiting the projection w.r.t. the \mathbf{K} -norm the shape of the cost function $\Theta_{j,k}(\mathbf{w}_{j,k})$ is changed such that convergence speed and steady-state performance are improved [53]. In comparison to central CHYPASS we can observe that D-CHYPASS nearly achieves its central benchmark performance.

D-CHYPASS (I) and (II) show a similar performance with

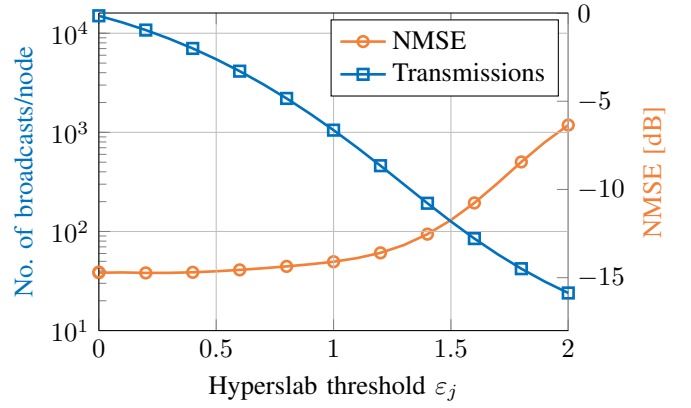


Fig. 2. Number of broadcast transmissions per node and NMSE for different values of the hyperslab threshold ε_j for the D-CHYPASS.

a negligible loss for D-CHYPASS (II). However, this minor loss comes with a huge reduction in complexity. Since D-CHYPASS (II) projects onto a hyperslab the probability that $\mathbf{w}_{j,k}$ is contained in the set $\mathcal{S}_{j,k}$ is significantly higher for $\varepsilon_j = 0.5$ than for $\varepsilon_j = 0$. Therefore, in case $\mathbf{w}_{j,k} \in \mathcal{S}_{j,k}$ the vector $\mathbf{w}_{j,k}$ is not updated and hence, does not need to be transmitted again to neighboring nodes. Obviously, this significantly reduces complexity and communication overhead. In contrast, when using a hyperplane with $\varepsilon_j = 0$ the vector $\mathbf{w}_{j,k}$ has to be updated in each iteration and thus, each coefficient vector has to be broadcast. Figure 2 shows the number of broadcast transmissions per node in logarithmic scale over the hyperslab threshold ε_j . Additionally, the NMSE averaged over the last 200 iterations in relation to the threshold is depicted. For thresholds $\varepsilon_j > 0$ a step size of $\mu_{j,k} = 0.5$ is used. We can observe that using hyperslab thresholds up to $\varepsilon_j = 0.5$ saves a huge amount of transmissions while keeping the error performance constant. E.g. for D-CHYPASS (II) with $\varepsilon_j = 0.5$ in average 5,468 transmissions are executed per node. Compared to 15,000 transmissions for D-CHYPASS (I) a reduction of approximately 64% in computations and communication overhead can be achieved. This is crucial especially for sensors with low computational capability and limited battery life. However, from Figure 2 it is also clear that the overhead cannot be arbitrarily reduced without degrading the reconstruction performance. This is visible especially for thresholds $\varepsilon_j > 1$.

In Figure 3 we depict the contour plot of the true function $\psi(\mathbf{x})$ together with an exemplary set of node positions and the reconstructed function $\varphi(\mathbf{x})$ by D-CHYPASS (I). The reconstruction is shown for one node in the network after steady state. By virtue of the consensus averaging step each node in the network will have the same reconstruction. We can observe that both Gaussian functions are approximated with good accuracy. The peaks of both functions can be clearly distinguished. However, at outer regions some inaccuracies can still be seen. These are expected to be reduced when increasing the dictionary size.

Figure 4 shows the error performance of the algorithms over the averaged dictionary size \bar{r} for 200 trials. The NMSE values

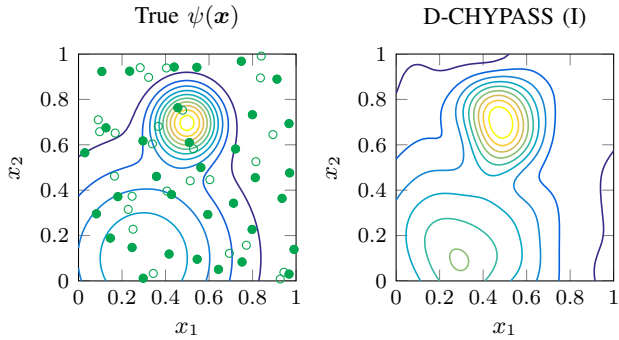


Fig. 3. Contour plots of the true $\psi(\mathbf{x})$ (left) and its reconstruction $\varphi(\mathbf{x})$ (right) at one node using the D-CHYPASS at steady state. Green circles show the node positions and filled circles the chosen dictionary entries.

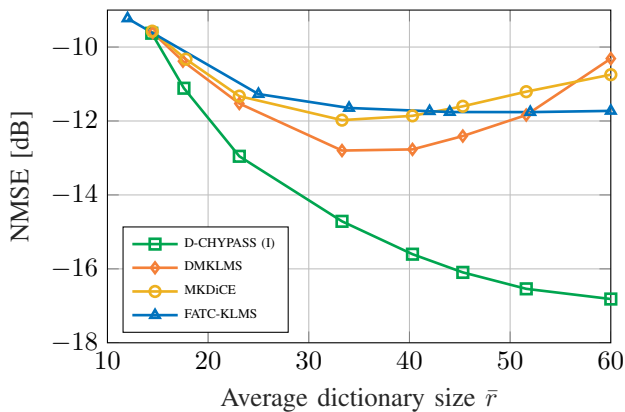


Fig. 4. NMSE over dictionary size for the reconstruction of multiple Gaussian functions.

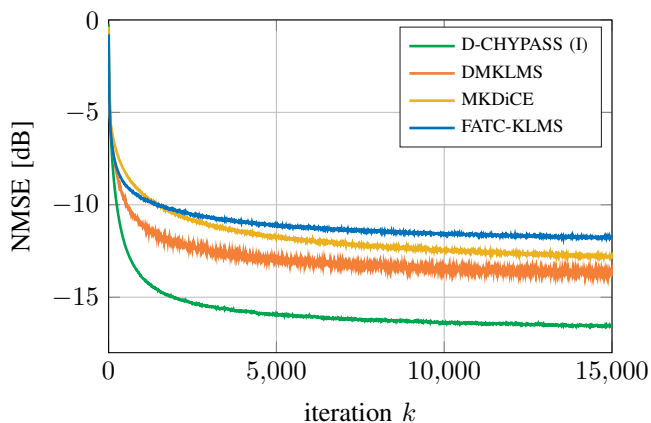


Fig. 5. Learning curves for the reconstruction of multiple Gaussian functions for a coherence threshold $\tau = 0.99$ corresponding to an average dictionary size of $\bar{r} = 53$ samples.

TABLE II
PARAMETER VALUES FOR EXPERIMENT IN SECTION V-B

Algorithm	Parameters		
D-CHYPASS	$\mu_{j,k} = 0.5, \varepsilon_j = 0$	$\tau = 0.85$	$\zeta_1 = 0.06$
DMKLMS	$\mu_{j,k} = 0.05$		$\zeta_2 = 0.1$
MKDiCE	$\mu_{j,k} = 0.7$	$\tau = 0.78$	$\zeta = 0.08$
FATC-KLMS	$\mu_{j,k} = 0.05$		
RFF-DKLMS	$\mu_{j,k} = 0.2$	$r_{\text{RFF}} = 200$	$\zeta = 0.08$

are calculated as an average over the last 200 iterations with again 15,000 iterations for each algorithm. We observe that D-CHYPASS (I) outperforms its competitors with growing dictionary size. In particular, DMKLMS and MKDiCE lose in performance for dictionary sizes $\bar{r} > 33$ while D-CHYPASS steadily improves its reconstruction. This is due to the reason that for DMKLMS and MKDiCE the step size has to be adjusted to the growing dictionary size to avoid an increasing steady-state error. In DMKLMS the step size is not normalized to the squared norm of the kernel vector $\kappa(\mathbf{x})$ as in D-CHYPASS which can lead to divergence. Regarding FATC-KLMS a similar effect is expected to appear for higher dictionary sizes $\bar{r} > 60$ since it uses one kernel only. Therefore, in the range of 40 to 60 dictionary samples it performs better than DMKLMS and MKDiCE. To show that the performance of MKDiCE and DMKLMS can be improved, in Figure 5 we depict the NMSE performance for an adapted step size over the iteration with $\tau = 0.99$. This coherence threshold results in an average dictionary size of $\bar{r} = 53$, a point where MKDiCE and DMKLMS show degrading performance according to Figure 4. The step sizes are chosen as $\mu_{j,k} = 0.05$ for DMKLMS and $\mu_{j,k} = 0.2$ for MKDiCE, respectively. We observe that by adjusting the step size to the dictionary size the steady-state performance at $\bar{r} = 53$ is improved compared to Figure 4. Now, both MKDiCE and DMKLMS outperform FATC-KLMS.

Remark 1: Regarding D-CHYPASS (I) it should be noted that for $\tau > 0.98$ divergence was observed. This is caused by the inversion of an ill-conditioned kernel Gram matrix \mathbf{K} . This occurs if the dictionary employs node positions close to each other leading to linear dependency in \mathbf{K} . With a higher coherence threshold the probability of such a case increases. To numerically stabilize the inversion of \mathbf{K} a scaled identity matrix $\gamma \mathbf{I}_{r_Q}$ is added to the matrix as regularization. The matrix \mathbf{K} in (14) is then substituted by $\mathbf{K} + \gamma \mathbf{I}_{r_Q}$. For thresholds $\tau > 0.98$ a regularization parameter of $\gamma = 0.01$ was used in this experiment to achieve a stable performance.

B. Real Altitude Data

We apply D-CHYPASS to the reconstruction of real altitude data where each node measures the altitude at its position \mathbf{x}_j . For the data we use the ETOPO1 global relief model which is provided by the National Oceanic and Atmospheric Administration [54] and which exhibits several low/high frequency components. In the original data the position is given by the longitude and latitude and the corresponding altitude $\psi(\mathbf{x})$ is delivered for each such position. As in [55], we choose an area

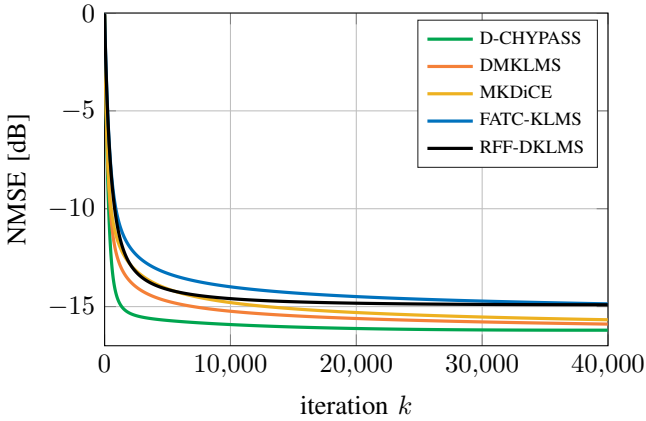


Fig. 6. Learning curves for the reconstruction of altitude data.

of 31×31 points with longitudes $\{138.5, 138.5 + \frac{1}{60}, \dots, 139\}$ and latitudes $\{34.5, 34.5 + \frac{1}{60}, \dots, 35\}$. However, for easier handling we map longitudes and latitudes to Cartesian coordinates in the unit-square area such that $\mathbf{x} \in [0, 1]^2$. We consider $J = 200$ randomly placed over the described area. Nodes with a distance $D < 0.2$ to each other share a connection. We assume noise with $\sigma_n^2 = 0.3$. The coherence threshold is set such that each algorithm employs a dictionary of average size $\bar{r} = 105$ while the RFF-DKLMS uses $r_{\text{RFF}} = 200$ Fourier features. The performances are averaged over 200 independent trials. Table II lists the chosen parameter values for the considered algorithms.

Figure 6 depicts the NMSE performance over the iteration. Again D-CHYPASS outperforms the other algorithms in terms of convergence speed and steady-state error. Although DMKLMS performs very close to D-CHYPASS it can be observed that the convergence speed of D-CHYPASS is faster. FATC-KLMS and RFF-DKLMS perform worst since their reconstruction capability is limited by the use of one kernel only. We see that RFF-DKLMS converges faster than FATC-KLMS. However, it should be noted that it produces a higher communication overhead due to the use of $r_{\text{RFF}} = 200$ Fourier features compared to $\bar{r} = 105$ dictionary samples in FATC-KLMS. The contour plots for the multikernel approaches at steady-state at one node are shown in Figure 7. For the D-CHYPASS we can observe a good reconstruction of the original $\psi(\mathbf{x})$ although details in the area around $[0.4, 0.7]^T$ and $[0.4, 0.3]^T$ are missing. The reconstructions by DMKLMS and MKDiCE show a less accurate approximation especially in the areas around the valley $[0.4, 0.3]^T$.

C. Time-Varying Function

In the following, we examine the tracking performance of the D-CHYPASS w.r.t. time-varying functions. To this end, we consider the following function being dependent on both the position \mathbf{x} and time k :

$$\psi(\mathbf{x}, k) = 0.8 \exp\left(-\frac{\|\mathbf{x} - \mathbf{p}_1\|_{\mathbb{R}^2}^2}{2(1 - 0.5 \sin(2\pi 10^{-3}k)) \cdot 0.3^2}\right) + \exp\left(-\frac{\|\mathbf{x} - \mathbf{p}_2\|_{\mathbb{R}^2}^2}{2(1 + 0.5 \sin(2\pi 10^{-3}k)) \cdot 0.1^2}\right)$$

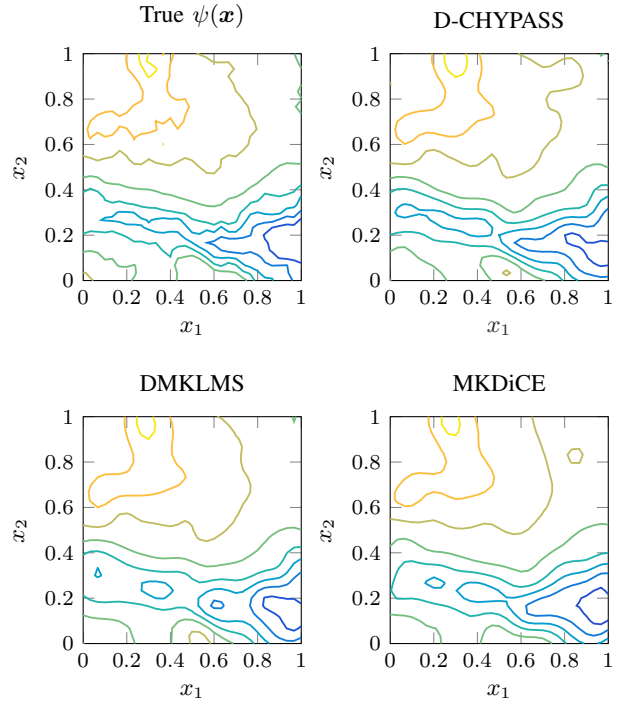


Fig. 7. Contour plots of the altitude reconstruction by one node for the D-CHYPASS, DMKLMS, and MKDiCE.

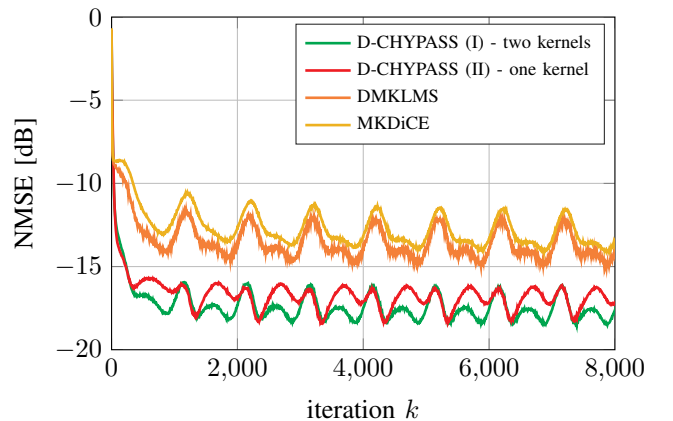


Fig. 8. NMSE performance over iteration number for the tracking of a time-varying function.

with $\mathbf{p}_1 = [0.6, 0.5]^T$ and $\mathbf{p}_2 = [0.25, 0.3]^T$. This function contains two Gaussian shapes whose bandwidths are expanding and shrinking over time k . We apply the D-CHYPASS to the reconstruction of the time-varying function $\psi(\mathbf{x}, k)$ and compare it to the MKDiCE and DMKLMS. We use a network of $J = 80$ randomly distributed over the unit-square area and average the performance over 200 trials with a new network realization in each trial. The noise variance is $\sigma_n^2 = 0.3$. For the considered algorithms we set τ such that an average dictionary size of $\bar{r} = 36$ samples is achieved. We evaluate the D-CHYPASS with one and two kernels. Table III lists the chosen parameter values for the considered algorithms.

Figure 8 shows the NMSE over the iteration number k . The fluctuations in the error curves are due to the time-varying

TABLE III
PARAMETER VALUES FOR EXPERIMENT IN SECTION V-C

Algorithm	Parameters
D-CHYPASS (I)	$\mu_{j,k} = 0.5$ $\tau = 0.95$ $\zeta_1 = 0.1, \zeta_2 = 0.3$ $\varepsilon_j = 0$
D-CHYPASS (II)	$\mu_{j,k} = 0.5$ $\tau = 0.9$ $\zeta_1 = 0.2$ $\varepsilon_j = 0$
DMKLMS	$\mu_{j,k} = 0.1$ $\tau = 0.95$ $\zeta_1 = 0.1, \zeta_2 = 0.3$
MKDICE	$\mu_{j,k} = 0.5$ $\tau = 0.95$ $\zeta_1 = 0.1, \zeta_2 = 0.3$

bandwidths in $\psi(\mathbf{x}, k)$. For all algorithms these fluctuations stay in a specific error range illustrating that the function $\psi(\mathbf{x}, k)$ can be tracked within a certain range of accuracy. We observe that D-CHYPASS (I) and (II) significantly outperform the remaining algorithms. Additionally, the range of the fluctuations in the error is lower for D-CHYPASS compared to the other algorithms. It is also visible that utilizing two kernels in D-CHYPASS (I) improves the tracking performance compared to using one kernel as in D-CHYPASS (II). Nevertheless it is worth noting, that even with only one kernel the D-CHYPASS (II) outperforms the multikernel approaches DMKLMS and MKDiCE illustrating the significant gain by employing the \mathbf{K} -norm in the derivation of the algorithm.

D. Computational Complexity and Communication Overhead

We analyze the complexities and communication overhead of the algorithms per iteration in the network. For the complexities we consider the number of multiplications and assume that Gaussian kernels are used as in (4). Furthermore, each dictionary \mathcal{D}_q is designed a priori, stays fixed over time k and is common to all nodes. Therefore, the kernel Gram matrix \mathbf{K} can be computed offline before the iterative process of D-CHYPASS avoiding an inversion in each iteration. Note that \mathbf{K} is block diagonal such that Q inversions of $r \times r$ matrices have to be computed. This results in a complexity of order $\mathcal{O}(JQr^3)$ in the network before D-CHYPASS starts iterating. To further reduce the complexity of D-CHYPASS the selective-update strategy can be applied which selects the s most coherent dictionary samples such that only s entries of the coefficient vector $\mathbf{w}_{j,k}$ are updated [47]. Usually, $s \leq 5$ so that $s \ll r$. Then per iteration k the inverse of an $s \times s$ matrix has to be computed while the complexity of the multiplications is heavily reduced. For the overhead we count the number of transmitted scalars among all nodes. All algorithms except the MKDiCE use a consensus averaging step which produces only broadcast transmissions. Beside broadcasts the MKDiCE comprises also unicast transmissions of vectors which depend on the receiving neighboring node and which increase the overhead significantly. Table IV lists the complexities and overhead of the algorithms where the complexity for an inversion of a $p \times p$ matrix is denoted by $v_{\text{inv}}(p) := p^3$. Figure 9 depicts the complexity and the overhead over the dictionary size r for $L = 2, s = 7, Q = 2$ and a network of $J = 60$ nodes with $|\mathcal{E}| = 300$ edges. The RFF-DKLMS with $r_{\text{RFF}} = 500$ is included as reference. It can be clearly seen that the complexity and overhead of the

ADMM-based MKDiCE are highest among the algorithms due to the inversion of a $Qr \times Qr$ matrix per iteration k and the transmission of unicast vectors, respectively. Furthermore, for dictionary sizes up to $r = 50$ the D-CHYPASS has lower complexity than the RFF-DKLMS. By including the selective-update strategy the complexity of D-CHYPASS is significantly reduced and is even lower than single kernel FATC-KLMS. D-CHYPASS and DMKLMS exhibit the same overhead per iteration which is lower compared to that of RFF-DKLMS for dictionary sizes up to $r = 200$. Note that the overall overhead of D-CHYPASS can be even further reduced when the hyperslab threshold is $\varepsilon_j > 0$ as shown in Figure 2.

TABLE IV
COMPUTATIONAL COMPLEXITY AND OVERHEAD OF ALGORITHMS

Algorithm	Complexity	Overhead
D-CHYPASS	$(2 \mathcal{E} + J(L+4))Qr$ $+ (Qr^2 + 2)J$	JQr
D-CHYPASS (selective update)	$((L+1)Qr + v_{\text{inv}}(s) + s^2 + 2)J$ $+ (2 \mathcal{E} + 3J)s$	
DMKLMS	$(2 \mathcal{E} + J(L+4))Qr + J$	
FATC-KLMS	$(2 \mathcal{E} + J(L+4))r + J$	Jr
MKDiCE	$(6 \mathcal{E} + 4J + L + 2)Qr$ $+ J(1 + (Qr)^2 + v_{\text{inv}}(Qr))$	$2JQr$ $+ 2 \mathcal{E} Qr$
RFF-DKLMS	$J(4r_{\text{RFF}} + 1) + (2 \mathcal{E} + J)r_{\text{RFF}}$	Jr_{RFF}

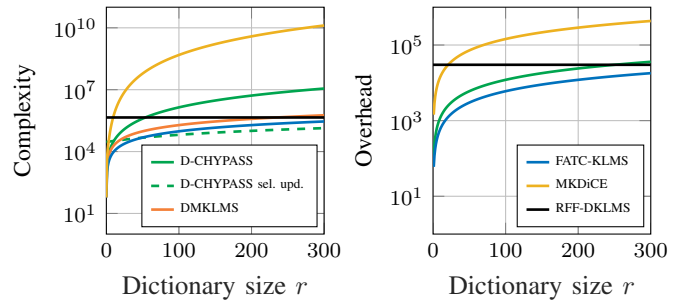


Fig. 9. Computational complexity and communication overhead of the algorithms per iteration k over the dictionary size r .

VI. CONCLUSION

We proposed an adaptive learning algorithm exploiting multiple kernels and projections onto hyperslabs for nonlinear system identification in diffusion networks. We provided a thorough convergence analysis regarding monotone approximation, asymptotic minimization, consensus and the limit point of the algorithm. To this end, we introduced a novel modified consensus matrix which we proved to be equivalent to the ordinary consensus matrix. As an application example we investigated the proposed scheme for the reconstruction of spatial distributions by a network of nodes with both synthetic and real data. Note that it is not restricted to such a scenario and can be applied in general to any distributed nonlinear system identification task. Compared to the state of the art algorithms we could observe significant gains in error performance, convergence speed and stability over the employed

dictionary size. In particular, our proposed APSM-based algorithm significantly outperformed an ADMM-based multikernel scheme (MKDiCE) in terms of error performance with highly decreased complexity and communication overhead. By embedding the hyperslab projection the communication overhead in the network as well as the computational complexity per node could be drastically reduced over a certain range of thresholds while keeping the error performance constant.

APPENDIX A PROOF OF LEMMA 2

Let us consider the squared \mathcal{K} -norm of $\widehat{\mathbf{P}}$:

$$\|\widehat{\mathbf{P}}\|_{\mathcal{K}}^2 := \max_{\mathbf{x} \neq \mathbf{0}} \frac{\|\widehat{\mathbf{P}}\mathbf{x}\|_{\mathcal{K}}^2}{\|\mathbf{x}\|_{\mathcal{K}}^2} = \max_{\mathbf{x} \neq \mathbf{0}} \frac{\mathbf{x}^\top \widehat{\mathbf{P}}^\top \mathcal{K} \widehat{\mathbf{P}} \mathbf{x}}{\mathbf{x}^\top \mathcal{K} \mathbf{x}}$$

We assume \mathcal{K} to be non-singular. Hence, $\mathcal{K}^{-1/2}$ exists and we can insert $\widehat{\mathbf{P}} = \mathcal{K}^{-1/2} \mathbf{P} \mathcal{K}^{1/2}$:

$$\begin{aligned} \|\widehat{\mathbf{P}}\|_{\mathcal{K}}^2 &= \max_{\mathbf{x} \neq \mathbf{0}} \frac{\mathbf{x}^\top \mathcal{K}^{1/2} \mathbf{P}^\top \mathcal{K}^{-1/2} \mathcal{K} \mathcal{K}^{-1/2} \mathbf{P} \mathcal{K}^{1/2} \mathbf{x}}{\mathbf{x}^\top \mathcal{K} \mathbf{x}} \\ &= \max_{\mathbf{y} \neq \mathbf{0}} \frac{\mathbf{y}^\top \mathbf{P}^\top \mathbf{P} \mathbf{y}}{\mathbf{y}^\top \mathbf{y}} \text{ with } \mathbf{y} = \mathcal{K}^{1/2} \mathbf{x} \end{aligned}$$

By definition of the consensus matrix \mathbf{P} it follows that $\|\widehat{\mathbf{P}}\|_{\mathcal{K}}^2 = 1$.

We show now that the modified consensus matrix $\widehat{\mathbf{P}}$ is equivalent to \mathbf{P} . Assume that \mathbf{P} is compatible to the graph \mathcal{G} of any connected, undirected network via the matrix $\mathbf{G} \in \mathbb{R}^{J \times J}$. Then, it holds that $\mathbf{P} = \mathbf{G} \otimes \mathbf{I}_{rQ}$. By examining the definition of $\widehat{\mathbf{P}}$ we find

$$\begin{aligned} \widehat{\mathbf{P}} &= \mathcal{K}^{-1/2} \mathbf{P} \mathcal{K}^{1/2} = \mathcal{K}^{-1/2} (\mathbf{G} \otimes \mathbf{I}_{rQ}) \mathcal{K}^{1/2} \\ &= \begin{bmatrix} \mathbf{K}^{-1/2} & & \mathbf{0} \\ & \ddots & \\ \mathbf{0} & & \mathbf{K}^{-1/2} \end{bmatrix} \\ &\times \begin{bmatrix} g_{11} \mathbf{I}_{rQ} & \dots & g_{1J} \mathbf{I}_{rQ} \\ \vdots & \ddots & \vdots \\ g_{J1} \mathbf{I}_{rQ} & \dots & g_{JJ} \mathbf{I}_{rQ} \end{bmatrix} \begin{bmatrix} \mathbf{K}^{1/2} & & \mathbf{0} \\ & \ddots & \\ \mathbf{0} & & \mathbf{K}^{1/2} \end{bmatrix} \\ &= \begin{bmatrix} g_{11} \mathbf{K}^{-1/2} \mathbf{I}_{rQ} \mathbf{K}^{1/2} & \dots & g_{1J} \mathbf{K}^{-1/2} \mathbf{I}_{rQ} \mathbf{K}^{1/2} \\ \vdots & \ddots & \vdots \\ g_{J1} \mathbf{K}^{-1/2} \mathbf{I}_{rQ} \mathbf{K}^{1/2} & \dots & g_{JJ} \mathbf{K}^{-1/2} \mathbf{I}_{rQ} \mathbf{K}^{1/2} \end{bmatrix} \\ &= \mathbf{G} \otimes \mathbf{I}_{rQ} = \mathbf{P} \end{aligned}$$

Thus, matrices $\widehat{\mathbf{P}}$ and \mathbf{P} are equivalent to each other.

APPENDIX B PROOF OF THEOREM 1

A. Proof of Theorem 1.1

By virtue of Lemma 2 it holds that $\|\mathbf{P}\|_2 = \|\mathbf{P}\|_{\mathcal{K}} = 1$. According to (19) we can express the D-CHYPASS via $\mathbf{z}_{k+1} = \mathbf{P}(\mathbf{z}_k - \Phi_k)$. Then, for the monotone approximation

we need to show that $\|\mathbf{z}_{k+1} - \mathbf{z}_k^*\|_{\mathcal{K}} < \|\mathbf{z}_k - \mathbf{z}_k^*\|_{\mathcal{K}}$. We have

$$\begin{aligned} &\|\mathbf{z}_{k+1} - \mathbf{z}_k^*\|_{\mathcal{K}}^2 \\ &= \|\mathbf{P}(\mathbf{z}_k - \Phi_k - \mathbf{z}_k^*)\|_{\mathcal{K}}^2 \\ &\leq \|\mathbf{P}\|_{\mathcal{K}}^2 \cdot \|\mathbf{z}_k - \Phi_k - \mathbf{z}_k^*\|_{\mathcal{K}}^2 \\ &= \|\mathbf{z}_k - \mathbf{z}_k^*\|_{\mathcal{K}}^2 - 2 \langle \Phi_k, \mathbf{z}_k - \mathbf{z}_k^* \rangle_{\mathcal{K}} + \|\Phi_k\|_{\mathcal{K}}^2 \\ &= \|\mathbf{z}_k - \mathbf{z}_k^*\|_{\mathcal{K}}^2 \\ &\quad - 2 \sum_{j \in \mathcal{J}} \mu_{j,k} \langle \mathbf{w}_{j,k} - P_{S_{j,k}}^{\mathbf{K}}(\mathbf{w}_{j,k}), \mathbf{w}_{j,k} - \mathbf{w}_k^* \rangle_{\mathbf{K}} \\ &\quad + \sum_{j \in \mathcal{J}} \mu_{j,k}^2 \|\mathbf{w}_{j,k} - P_{S_{j,k}}^{\mathbf{K}}(\mathbf{w}_{j,k})\|_{\mathbf{K}}^2 \end{aligned}$$

From Theorem 3.14 in [56] we know that $\langle \mathbf{w}_{j,k} - P_{S_{j,k}}^{\mathbf{K}}(\mathbf{w}_{j,k}), \mathbf{w}_k^* - P_{S_{j,k}}^{\mathbf{K}}(\mathbf{w}_{j,k}) \rangle_{\mathbf{K}} \leq 0$ with $\mathbf{w}_k^* \in \mathcal{S}_{j,k}$. Therefore

$$\begin{aligned} &\langle \mathbf{w}_{j,k} - P_{S_{j,k}}^{\mathbf{K}}(\mathbf{w}_{j,k}), \mathbf{w}_k^* \rangle_{\mathbf{K}} \leq \\ &\langle \mathbf{w}_{j,k} - P_{S_{j,k}}^{\mathbf{K}}(\mathbf{w}_{j,k}), P_{S_{j,k}}^{\mathbf{K}}(\mathbf{w}_{j,k}) \rangle_{\mathbf{K}} \end{aligned}$$

and thus

$$\langle \mathbf{w}_{j,k} - P_{S_{j,k}}^{\mathbf{K}}(\mathbf{w}_{j,k}), \mathbf{w}_{j,k} - \mathbf{w}_k^* \rangle_{\mathbf{K}} \geq \|\mathbf{w}_{j,k} - P_{S_{j,k}}^{\mathbf{K}}(\mathbf{w}_{j,k})\|_{\mathbf{K}}^2.$$

Then, it follows that

$$\begin{aligned} &\|\mathbf{z}_{k+1} - \mathbf{z}_k^*\|_{\mathcal{K}}^2 \\ &\leq \|\mathbf{z}_k - \mathbf{z}_k^*\|_{\mathcal{K}}^2 - 2 \sum_{j \in \mathcal{J}} \mu_{j,k} \|\mathbf{w}_{j,k} - P_{S_{j,k}}^{\mathbf{K}}(\mathbf{w}_{j,k})\|_{\mathbf{K}}^2 \\ &\quad + \sum_{j \in \mathcal{J}} \mu_{j,k}^2 \|\mathbf{w}_{j,k} - P_{S_{j,k}}^{\mathbf{K}}(\mathbf{w}_{j,k})\|_{\mathbf{K}}^2 \\ &= \|\mathbf{z}_k - \mathbf{z}_k^*\|_{\mathcal{K}}^2 \\ &\quad - \sum_{j \in \mathcal{J}} (2 - \mu_{j,k}) \mu_{j,k} \|\mathbf{w}_{j,k} - P_{S_{j,k}}^{\mathbf{K}}(\mathbf{w}_{j,k})\|_{\mathbf{K}}^2 \end{aligned}$$

Since $\|\mathbf{w}_{j,k} - P_{S_{j,k}}^{\mathbf{K}}(\mathbf{w}_{j,k})\|_{\mathbf{K}}^2 > 0$ ($\Leftrightarrow \mathbf{w}_{j,k} \notin \mathcal{S}_{j,k}$) and $\mu_{j,k} \in (0, 2)$ for at least one node j and $\mu_{i,k} \in [0, 2]$ for $j \neq i$, we can conclude that $\|\mathbf{z}_{k+1} - \mathbf{z}_k^*\|_{\mathcal{K}} < \|\mathbf{z}_k - \mathbf{z}_k^*\|_{\mathcal{K}}$ which completes the proof. The corresponding proof from [10, Theorem (1a)] holds true for $\|\mathbf{P}\|_{\mathcal{K}} = 1$.

B. Proof of Theorem 1.2

From Theorem 1.1 we know that the sequence $(\|\mathbf{z}_k - \mathbf{z}^*\|_{\mathcal{K}})_{k \in \mathbb{N}}$ is monotonically decreasing and bounded below. Thus, it converges and we deduce that

$$\begin{aligned} &\lim_{k \rightarrow \infty} (\|\mathbf{z}_k - \mathbf{z}^*\|_{\mathcal{K}}^2 - \|\mathbf{z}_{k+1} - \mathbf{z}^*\|_{\mathcal{K}}^2) = 0 \\ &\Rightarrow \lim_{k \rightarrow \infty} \sum_{j \in \mathcal{J}} (2 - \mu_{j,k}) \mu_{j,k} \|\mathbf{w}_{j,k} - P_{S_{j,k}}^{\mathbf{K}}(\mathbf{w}_{j,k})\|_{\mathbf{K}}^2 = 0 \\ &\Leftrightarrow \lim_{k \rightarrow \infty} \sum_{j \in \mathcal{J}} (2 - \mu_{j,k}) \mu_{j,k} \Theta_{j,k}^2(\mathbf{w}_{j,k}) = 0 \end{aligned}$$

With $\mu_{j,k} \in [\epsilon_1, 2 - \epsilon_2]$ it follows that the local costs $\Theta_{j,k}(\mathbf{w}_{j,k}) = \|\mathbf{w}_{j,k} - P_{S_{j,k}}^{\mathbf{K}}(\mathbf{w}_{j,k})\|_{\mathbf{K}}$ are asymptotically minimized for every $j \in \mathcal{J}$.

C. Proof of Theorem 1.3

The proof mainly follows the proofs given in Appendix II and Appendix III of [10]. However, for the D-CHYPASS we need to consider the \mathcal{K} -norm. By virtue of the equivalence of norms (see Appendix 1.4 in [46]) for any vector $\mathbf{x} \in \mathbb{R}^{rQJ}$ it holds that

$$\alpha \|\mathbf{x}\|_{\mathbb{R}^{rQJ}} \leq \|\mathbf{x}\|_{\mathcal{K}} \leq \beta \|\mathbf{x}\|_{\mathbb{R}^{rQJ}}$$

for some positive constants $0 < \alpha \leq \beta < \infty$. From [10, Appendix III] we have that $\lim_{k \rightarrow \infty} \|\Phi_k\|_{\mathbb{R}^{rQJ}} = 0$ which implies $\lim_{k \rightarrow \infty} \|\Phi_k\|_{\mathcal{K}} = 0$. Consequently, the proofs in Appendix II and Appendix III of [10] regarding the asymptotic consensus hold for the \mathcal{K} -norm as well and are therefore not repeated here.

D. Proof of Theorem 1.4

We mimic the proof of [49, Theorem 2.3] to show the convergence of $(\mathbf{z}_k)_{k \in \mathbb{N}}$. From Theorem 1.1 we know that the sequence $(\|\mathbf{z}_k - \mathbf{z}^*\|_{\mathcal{K}}^2)_{k \in \mathbb{N}}$ converges for every $\mathbf{z}^* = [(\mathbf{w}^*)^\top, \dots, (\mathbf{w}^*)^\top]^\top$ where $\mathbf{w}^* \in \Upsilon^*$. Thus, the sequence $(\mathbf{z}_k)_{k \in \mathbb{N}}$ is bounded and every subsequence of $(\mathbf{z}_k)_{k \in \mathbb{N}}$ has an accumulation point. Then, according to the Bolzano-Weierstrass Theorem the bounded real sequence $(\mathbf{z}_k)_{k \in \mathbb{N}}$ has a convergent subsequence $(\mathbf{z}_{k_l})_{k_l \in \mathbb{N}}$. Let $\hat{\mathbf{z}}$ be the unique accumulation point of $(\mathbf{z}_{k_l})_{k_l \in \mathbb{N}}$. With $\lim_{k \rightarrow \infty} (\mathbf{I}_{rQJ} - \mathbf{B}\mathbf{B}^\top) \mathbf{z}_k = \mathbf{0}$ it follows that

$$\lim_{k \rightarrow \infty} (\mathbf{I}_{rQJ} - \mathbf{B}\mathbf{B}^\top) \mathbf{z}_{k_l} = (\mathbf{I}_{rQJ} - \mathbf{B}\mathbf{B}^\top) \hat{\mathbf{z}} = \mathbf{0}.$$

Hence, $\hat{\mathbf{z}}$ lies in the consensus subspace \mathcal{C} . To show that this point is a unique accumulation point suppose the contrary, i.e., $\hat{\mathbf{z}} = [\hat{\mathbf{w}}^\top, \dots, \hat{\mathbf{w}}^\top]^\top \in \mathcal{C}$ and $\tilde{\mathbf{z}} = [\tilde{\mathbf{w}}^\top, \dots, \tilde{\mathbf{w}}^\top]^\top \in \mathcal{C}$ are two different accumulation points. For every \mathbf{z}^* the sequence $(\|\mathbf{z}_k - \mathbf{z}^*\|_{\mathcal{K}}^2)_{k \in \mathbb{N}}$ converges and hence it follows that

$$\begin{aligned} 0 &= \|\hat{\mathbf{z}} - \mathbf{z}^*\|_{\mathcal{K}}^2 - \|\tilde{\mathbf{z}} - \mathbf{z}^*\|_{\mathcal{K}}^2 \\ &= \|\hat{\mathbf{z}}\|_{\mathcal{K}}^2 - \|\tilde{\mathbf{z}}\|_{\mathcal{K}}^2 - 2(\hat{\mathbf{z}} - \tilde{\mathbf{z}})^\top \mathcal{K} \mathbf{z}^* \\ &= \|\hat{\mathbf{z}}\|_{\mathcal{K}}^2 - \|\tilde{\mathbf{z}}\|_{\mathcal{K}}^2 - 2J(\hat{\mathbf{w}} - \tilde{\mathbf{w}})^\top \mathbf{K} \mathbf{w}^*. \end{aligned}$$

It thus holds that $\mathbf{w}^* \in H := \{\mathbf{w} \mid 2J(\hat{\mathbf{w}} - \tilde{\mathbf{w}})^\top \mathbf{K} \mathbf{w} = \|\hat{\mathbf{z}}\|_{\mathcal{K}}^2 - \|\tilde{\mathbf{z}}\|_{\mathcal{K}}^2\}$ where $\hat{\mathbf{w}} - \tilde{\mathbf{w}} \neq \mathbf{0}$ ($\Leftrightarrow \hat{\mathbf{z}} \neq \tilde{\mathbf{z}}$). Since we assume that $\mathbf{w}^* \in \Upsilon^*$ this implies that Υ^* is a subset of the hyperplane H . This contradicts the assumption of a nonempty interior of Υ^* . Hence, the bounded sequence $(\mathbf{z}_k)_{k \in \mathbb{N}}$ has a unique accumulation point, and so it converges.

E. Proof of Theorem 1.5

In this proof we mimic the proof of [27, Theorem 2(d)], [57, Theorem 3.1.4] and [8, Theorem 2(e)] to characterize the limit point $\hat{\mathbf{w}}$ of the sequence $(\mathbf{w}_{j,k})_{k \in \mathbb{N}}, \forall j \in \mathcal{J}$. Furthermore, we need Claim 2 of [27] which is proven for any real Hilbert space and thus, also holds for the \mathbf{K} -metric Euclidean space considered here.

Fact 1 (Claim 2 in [27]): Let $C \subset \mathbb{R}^{rQ}$ be a nonempty closed convex set. Suppose that $\rho > 0$ and $\tilde{\mathbf{u}}$ satisfies $\{\mathbf{v} \in \mathbb{R}^{rQ} \mid \|\mathbf{v} - \tilde{\mathbf{u}}\|_{\mathcal{K}} \leq \rho\} \subset C$. Assume $\mathbf{w} \in \mathbb{R}^{rQ}/C$ and $t \in (0, 1)$ such that $\mathbf{u}_t := t\mathbf{w} + (1-t)\tilde{\mathbf{u}} \notin C$. Then $d_{\mathcal{K}}(\mathbf{w}, C) > \rho \frac{1-t}{t} = \rho \frac{\|\mathbf{u}_t - \mathbf{w}\|_{\mathcal{K}}}{\|\mathbf{u}_t - \tilde{\mathbf{u}}\|_{\mathcal{K}}} > 0$.

Assume the contrary of our statement, i.e., $\hat{\mathbf{w}} \notin \liminf_{k \rightarrow \infty} \Upsilon_k$. Denote by $\tilde{\mathbf{u}}$ an interior point of Υ^* . Therefore, there exists $\rho > 0$ such that $\{\mathbf{v} \in \mathbb{R}^{rQ} \mid \|\mathbf{v} - \tilde{\mathbf{u}}\|_{\mathcal{K}} \leq \rho\} \subset \Upsilon^*$. Furthermore, there exists $t \in (0, 1)$ such that $\mathbf{u}_t := t\hat{\mathbf{w}} + (1-t)\tilde{\mathbf{u}} \notin \Upsilon \supset \liminf_{k \rightarrow \infty} \Upsilon_k$. Since $\lim_{k \rightarrow \infty} \mathbf{w}_{j,k} = \hat{\mathbf{w}} (\forall j \in \mathcal{J})$ there exists $N_1 \in \mathbb{N}$ such that $\|\mathbf{w}_{j,k} - \hat{\mathbf{w}}\|_{\mathcal{K}} \leq \rho \frac{1-t}{2t}, \forall k \geq N_1, \forall j \in \mathcal{J}$. Then, by $\mathbf{u}_t \notin \liminf_{k \rightarrow \infty} \Upsilon_k$ for any $L_1 > N_1$ there exists $k_1 \geq L_1$ satisfying $\mathbf{u}_t \notin \Upsilon_{k_1} = \bigcap_{j \in \mathcal{J}} (\text{lev}_{\leq 0} \Theta_{j,k_1})$. It follows that there exists a node $i \in \mathcal{J}$ such that $\mathbf{u}_t \notin \text{lev}_{\leq 0} \Theta_{i,k_1}$. By $\Upsilon \subset \Upsilon_k \subset \text{lev}_{\leq 0} \Theta_{i,k_1}$ and Fact 1 for node i it holds that

$$\begin{aligned} d_{\mathcal{K}}(\mathbf{w}_{i,k_1}, \text{lev}_{\leq 0} \Theta_{i,k_1}) &\geq d_{\mathcal{K}}(\hat{\mathbf{w}}, \text{lev}_{\leq 0} \Theta_{i,k_1}) \\ &\quad - \|\mathbf{w}_{i,k_1} - \hat{\mathbf{w}}\|_{\mathcal{K}} \\ &\geq \rho \frac{1-t}{t} - \frac{\rho}{2} \frac{1-t}{t} \\ &= \frac{\rho}{2} \frac{1-t}{t} =: \epsilon > 0 \end{aligned}$$

Thus, it follows that $\sum_{j \in \mathcal{J}} d_{\mathcal{K}}(\mathbf{w}_{j,k_1}, \text{lev}_{\leq 0} \Theta_{j,k_1}) \geq \epsilon$. By the triangle inequality we have

$$\begin{aligned} \|\tilde{\mathbf{u}} - \mathbf{w}_{j,k_1}\|_{\mathcal{K}} &\leq \|\tilde{\mathbf{u}} - \hat{\mathbf{w}}\|_{\mathcal{K}} + \|\mathbf{w}_{j,k_1} - \hat{\mathbf{w}}\|_{\mathcal{K}} \\ &\leq \|\tilde{\mathbf{u}} - \hat{\mathbf{w}}\|_{\mathcal{K}} + \frac{\rho}{2} \frac{1-t}{t} \quad (j \in \mathcal{J}) \end{aligned}$$

so that

$$\sum_{j \in \mathcal{J}} \|\tilde{\mathbf{u}} - \mathbf{w}_{j,k_1}\|_{\mathcal{K}} \leq J \|\tilde{\mathbf{u}} - \hat{\mathbf{w}}\|_{\mathcal{K}} + J \frac{\rho}{2} \frac{1-t}{t} =: \eta > 0.$$

Given a fixed $L_2 > k_1$, we can find a $k_2 \geq L_2$ such that $\sum_{j \in \mathcal{J}} d_{\mathcal{K}}(\mathbf{w}_{j,k_2}, \text{lev}_{\leq 0} \Theta_{j,k_2}) \geq \epsilon$ and $\sum_{j \in \mathcal{J}} \|\tilde{\mathbf{u}} - \mathbf{w}_{j,k_2}\|_{\mathcal{K}} \leq \eta$. Thus, we can construct a subsequence $\{k_l\}_{l=1}^{\infty}$ satisfying

$$\sum_{j \in \mathcal{J}} d_{\mathcal{K}}(\mathbf{w}_{j,k_l}, \text{lev}_{\leq 0} \Theta_{j,k_l}) \geq \epsilon \quad \text{and} \quad \sum_{j \in \mathcal{J}} \|\tilde{\mathbf{u}} - \mathbf{w}_{j,k_l}\|_{\mathcal{K}} \leq \eta.$$

With the assumptions of the theorem there exists a $\zeta > 0$ such that $\sum_{j \in \mathcal{J}} \Theta_{j,k_l}(\mathbf{w}_{j,k_l}) \geq \zeta$ for every $l \geq 1$. However, this contradicts $\lim_{k \rightarrow \infty} \Theta_{j,k}(\mathbf{w}_{j,k}) = 0, \forall j \in \mathcal{J}$ from Theorem 1.2. Thus, it follows that $\hat{\mathbf{w}} \in \liminf_{k \rightarrow \infty} \Upsilon_k$ and the proof is complete.

REFERENCES

- [1] M. U. Ilyas, M. Zubair Shafiq, A. X. Liu, and H. Radha, "A distributed algorithm for identifying information hubs in social networks," *IEEE J. Sel. Areas Commun.*, vol. 31, no. 9, pp. 629–640, 2013.
- [2] F. Ingelrest, G. Barrenetxea, G. Schaefer, M. Vetterli, O. Couach, and M. Parlange, "SensorScope," *ACM Transactions on Sensor Networks*, vol. 6, no. 2, pp. 1–32, February 2010.
- [3] F. Facchinei, S. Sagratella, and G. Scutari, "Parallel algorithms for big data optimization," *IEEE Trans. Signal Process.*, vol. 63, no. 7, 2015.
- [4] A. H. Sayed, "Adaptive networks," *Proc. IEEE*, vol. 102, no. 4, pp. 460–497, April 2014.
- [5] H. Paul, J. Fliege, and A. Dekorsy, "In-network-processing: Distributed consensus-based linear estimation," *IEEE Commun. Lett.*, vol. 17, no. 1, pp. 59–62, 2013.
- [6] G. Mateos and G. B. Giannakis, "Distributed recursive least-squares: Stability and performance analysis," *IEEE Trans. Signal Process.*, vol. 60, no. 7, pp. 3740–3754, July 2012.
- [7] S. Tu and A. H. Sayed, "Mobile adaptive networks," *IEEE J. Sel. Topics Signal Process.*, vol. 5, no. 4, pp. 649–664, August 2011.

- [8] R. L. G. Cavalcante, A. Rogers, N. R. Jennings, and I. Yamada, "Distributed asymptotic minimization of sequences of convex functions by a broadcast adaptive subgradient method," *IEEE J. Sel. Topics Signal Process.*, vol. 5, pp. 1–37, 2011.
- [9] F. Cattivelli and A. H. Sayed, "Diffusion LMS strategies for distributed estimation," *IEEE Trans. Signal Process.*, vol. 58, no. 3, pp. 1035–1048, 2010.
- [10] R. L. G. Cavalcante, I. Yamada, and B. Mulgrew, "An adaptive projected subgradient approach to learning in diffusion networks," *IEEE Trans. Signal Process.*, vol. 57, no. 7, pp. 2762–2774, 2009.
- [11] H. Zhu, A. Cano, and G. Giannakis, "Distributed consensus-based demodulation: algorithms and error analysis," *IEEE Trans. Wireless Commun.*, vol. 9, no. 6, pp. 2044–2054, 2010.
- [12] I. D. Schizas, G. Mateos, and G. B. Giannakis, "Distributed LMS for consensus-based in-network adaptive processing," *IEEE Trans. Signal Process.*, vol. 57, no. 6, pp. 2365–2382, 2009.
- [13] B. Schölkopf and A. J. Smola, *Learning with Kernels: Support Vector Machines, Regularization, Optimization, and Beyond*. Cambridge, MA, USA: MIT Press, 2001.
- [14] T. Hofmann, B. Schölkopf, and A. J. Smola, "Kernel methods in machine learning," *The Annals of Statistics*, vol. 36, no. 3, pp. 1171–1220, jun 2008.
- [15] J. Kivinen, A. J. Smola, and R. C. Williamson, "Online learning with kernels," *IEEE Trans. Signal Process.*, vol. 52, no. 8, pp. 2165–2176, 2004.
- [16] Y. Engel, S. Mannor, and R. Meir, "The kernel recursive least-squares algorithm," *IEEE Trans. Signal Process.*, vol. 52, no. 8, pp. 2275–2285, August 2004.
- [17] S. Van Vaerenbergh, J. Via, and I. Santamaria, "A sliding-window kernel RLS algorithm and its application to nonlinear channel identification," in *IEEE ICASSP*, vol. 5, 2006.
- [18] W. Liu, P. Pokharel, and J. Principe, "The kernel least-mean-square algorithm," *IEEE Trans. Signal Process.*, vol. 56, no. 2, pp. 543–554, 2008.
- [19] W. Liu, I. M. Park, Y. Wang, and J. C. Principe, "Extended kernel recursive least squares algorithm," *IEEE Trans. Signal Process.*, vol. 57, no. 10, August 2009.
- [20] C. Richard, J. C. M. Bermudez, and P. Honeine, "Online prediction of time series data with kernels," *IEEE Trans. Signal Process.*, vol. 57, no. 3, 2009.
- [21] W. Liu, J. C. Principe, and S. Haykin, *Kernel Adaptive Filtering*. John Wiley & Sons, 2010.
- [22] S. Van Vaerenbergh, M. Lazaro-Gredilla, and I. Santamaria, "Kernel recursive least-squares tracker for time-varying regression," *IEEE Trans. Neural Netw. Learn. Syst.*, vol. 23, no. 8, pp. 1313–1326, August 2012.
- [23] M. Yukawa and R.-I. Ishii, "An efficient kernel adaptive filtering algorithm using hyperplane projection along affine subspace," in *EUSIPCO*, 2012, pp. 2183–2187.
- [24] W. Gao, J. Chen, C. Richard, J. Huang, and R. Flamary, "Kernel LMS algorithm with forward-backward splitting for dictionary learning," in *IEEE ICASSP*, 2013, pp. 5735–5739.
- [25] W. Gao and C. Richard, "Convex combinations of kernel adaptive filters," in *IEEE MLSP*, 2014.
- [26] M. Takizawa and M. Yukawa, "Adaptive nonlinear estimation based on parallel projection along affine subspaces in reproducing kernel hilbert space," *IEEE Trans. Signal Process.*, vol. 63, no. 16, pp. 4257–4269, 2015.
- [27] I. Yamada and N. Ogura, "Adaptive projected subgradient method for asymptotic minimization of sequence of nonnegative convex functions," *Numer. Funct. Anal. Optim.*, vol. 25, no. 7-8, pp. 593–617, 2004.
- [28] P. L. Combettes, "The foundations of set theoretic estimation," *Proceedings of the IEEE*, vol. 81, no. 2, pp. 182–208, 1993.
- [29] S. Theodoridis, K. Slavakis, and I. Yamada, "Adaptive learning in a world of projections," *IEEE Signal Process. Mag.*, vol. 28, no. 1, pp. 97–123, 2011.
- [30] M. Yukawa and K. R. Muller, "Why does a Hilbertian metric work efficiently in online learning with kernels?" *IEEE Signal Process. Lett.*, vol. 23, no. 10, pp. 1424–1428, 2016.
- [31] M. Yukawa, "Multikernel adaptive filtering," *IEEE Trans. on Signal Process.*, vol. 60, pp. 4672–4682, 2012.
- [32] —, "Adaptive learning in Cartesian product of reproducing kernel Hilbert spaces," *IEEE Trans. Signal Process.*, vol. 63, 2015.
- [33] B.-S. Shin, H. Paul, and A. Dekorsy, "Distributed kernel least squares for nonlinear regression applied to sensor networks," in *EUSIPCO*, 2016.
- [34] B.-S. Shin, H. Paul, M. Yukawa, and A. Dekorsy, "Distributed nonlinear regression with multiple Gaussian kernels," in *IEEE SPAWC*, 2017.
- [35] W. Gao, J. Chen, C. Richard, and J. Huang, "Diffusion adaptation over networks with kernel least-mean-square," in *IEEE CAMSAP*, 2015.
- [36] P. Bouboulis, S. Chouvardas, and S. Theodoridis, "Online distributed learning over networks in RKH spaces using random fourier features," *arXiv:1703.08131 [cs.LG]*, 2017.
- [37] S. Chouvardas and M. Draief, "A diffusion kernel LMS algorithm for nonlinear adaptive networks," in *IEEE ICASSP*, March 2016.
- [38] P. Honeine, C. Richard, J. C. M. Bermudez, H. Snoussi, M. Essoloh, and F. Vincent, "Functional estimation in Hilbert space for distributed learning in wireless sensor networks," in *IEEE ICASSP*, 2009.
- [39] P. Honeine, C. Richard, J. C. M. Bermudez, J. Chen, and H. Snoussi, "A decentralized approach for nonlinear prediction of time series data in sensor networks," *EURASIP J Wirel Commun Netw*, vol. 2010, no. 1, 2010.
- [40] J. Predd, S. Kulkarni, and H. Poor, "Distributed learning in wireless sensor networks," *IEEE Signal Process. Mag.*, pp. 56–69, 2006.
- [41] P. A. Forero, A. Cano, and G. B. Giannakis, "Consensus-based distributed support vector machines," *Journal of Machine Learning Research*, vol. 11, 2010.
- [42] S. Boyd, N. Parikh, E. Chu, B. Peleato, and J. Eckstein, "Distributed optimization and statistical learning via the alternating direction method of multipliers," *Foundations and Trends in Machine Learning*, vol. 3, no. 1, pp. 1–122, 2010.
- [43] R. A. Horn and C. R. Johnson, *Matrix analysis*. Cambridge University Press, 2013.
- [44] H. Stark and Y. Yang, *Vector space projections: a numerical approach to signal and image processing, neural nets, and optics*. Wiley, 1998.
- [45] D. G. Luenberger, *Optimization by Vector Space Methods*. John Wiley & Sons, 1969, vol. 41, no. 162.
- [46] S. Boyd and L. Vandenberghe, *Convex Optimization*, C. U. Press, Ed. Cambridge University Press, 2010, vol. 25, no. 3.
- [47] M. Takizawa and M. Yukawa, "Efficient dictionary-refining kernel adaptive filter with fundamental insights," *IEEE Trans. Signal Process.*, vol. 64, no. 16, pp. 4337–4350, August 2016.
- [48] I. Yamada, K. Slavakis, and K. Yamada, "An efficient robust adaptive filtering algorithm based on parallel subgradient projection techniques," *IEEE Trans. Signal Process.*, vol. 50, no. 5, pp. 1091–1101, 2002.
- [49] R. L. G. Cavalcante and S. Stanczak, "A distributed subgradient method for dynamic convex optimization problems under noisy information exchange," *IEEE J. Sel. Topics Signal Process.*, vol. 7, no. 2, pp. 243–256, 2013.
- [50] L. Xiao and S. Boyd, "Fast linear iterations for distributed averaging," *Systems & Control Letters*, vol. 53, no. 1, pp. 65–78, 2004.
- [51] S. Boyd and S. Lall, "A scheme for robust distributed sensor fusion based on average consensus," in *ISPN*, 2005, pp. 63–70.
- [52] L. Xiao, S. Boyd, and S.-J. Kim, "Distributed average consensus with least-mean-square deviation," *Journal of Parallel and Distributed Computing*, vol. 67, no. 1, pp. 33–46, 2007.
- [53] M. Yukawa, K. Slavakis, and I. Yamada, "Adaptive parallel quadratic-metric projection algorithms," *IEEE Trans. Audio, Speech, Language Process.*, vol. 15, no. 5, pp. 1665–1680, 2007.
- [54] C. Amante and B. Eakins, "Etopo1 1 arc-minute global relief model: Procedures, data sources and analysis," *NOAA Technical Memorandum NESDIS NGDC-24. National Geophysical Data Center, NOAA*, 2009.
- [55] O. Toda and M. Yukawa, "Online model-selection and learning for nonlinear estimation based on multikernel adaptive filtering," *IEICE Transactions on Fundamentals of Electronics, Communications and Computer Sciences*, vol. E100-A, no. 1, pp. 236–250, 2017.
- [56] H. H. Bauschke and P. L. Combettes, *Convex analysis and monotone operator theory in Hilbert spaces*. Springer, 2011, vol. 408.
- [57] "The adaptive projected subgradient method over the fixed point set of strongly attracting nonexpansive mappings," *Numerical Functional Analysis and Optimization*, vol. 27, no. 7-8, pp. 905–930, 2006.